Rheology of Miscible Polymer Blends with Hydrogen Bonding

Zhiyi Yang and Chang Dae Han*

Department of Polymer Engineering, The University of Akron, Akron, Ohio 44325

Received November 14, 2007; Revised Manuscript Received January 11, 2008

ABSTRACT: Linear dynamic viscoelasticity of miscible polymer blends with hydrogen bonding has been investigated. The polymer blend systems investigated are (1) blends of poly(vinylphenol) (PVPh) and poly(vinyl acetate) (PVAc), (2) blends of PVPh and poly(vinyl methyl ether) (PVME), (3) blends of PVPh and poly(2-vinylpyridine) (P2VP), and (4) blends of PVPh and poly(4-vinylpyridine) (P4VP). Fourier transform infrared (FTIR) spectroscopy was employed to find that both the intraassociation (self-association) of the phenolic −OH groups in PVPh and interassociation (intermolecular interactions) between the constituent components in each blend system have profound influence on the frequency dependence of dynamic moduli in the terminal region of the PVPh-based miscible blend systems. It has been found further that time−temperature superposition (TTS) is applicable to all four PVPh-based miscible blend systems forming hydrogen bonds, including the PVPh/PVME blends having the difference in component glass transition temperature (ΔT_g) as large as 199 °C. This observation is quite different from the experimental observations in the literature, reporting that TTS failed for miscible polymer blends *without* specific interaction when ΔT_g was greater than about 25 °C and the presence of concentration fluctuations and dynamic heterogeneity caused the failure of TTS. The experimental observations made from the present study suggest that the presence of concentration fluctuations and dynamic heterogeneity in the PVPh-based miscible blends forming hydrogen bonds (intermolecular interactions) between the constituent components might be very small, if not negligible.

1. Introduction

In the literature there is confusion about the criteria for weak attractive interaction and strong attractive interaction when dealing with miscible polymer blends. Often, the strength of miscibility of a polymer blend is judged using the Flory−Huggins interaction parameter (χ). For instance, some investigators consider that miscible polymer blends with $\chi = -0.05$ have strong attractive interaction while miscible polymer blends with $\chi = -0.01$ have weak attractive interaction. However, such a criterion is somewhat arbitrary in that there is no theoretical guideline on a precise value of χ that can be used effectively for determining whether a miscible polymer blend has weak or strong attractive interactions. In this regard, it is fair to say that χ may not be an appropriate parameter that can determine whether a miscible polymer blend has weak or strong attractive interactions.

It seems more appropriate to use intermolecular forces to determine whether a miscible polymer blend has weak or strong attractive interactions. Intermolecular forces have been discussed extensively in the literature.[1,2] Table 1 gives a summary of bond energy and relative strength of different intermolecular forces. On the basis of the intermolecular forces summarized in Table 1, in this paper we consider that the miscible polymer blends with van der Waals interaction (i.e., without specific interaction) have weak attractive interaction and the miscible polymer blends with specific interaction (e.g., dipole−dipole interaction, hydrogen bonding, or ionic interaction) have strong attractive interaction. It should be mentioned that specific interaction in a miscible polymer blends cannot be described by the Flory−Huggins theory and thus not by the use of χ.

During the past three decades, numerous investigators reported on the rheological behavior of miscible polymer blends without specific interaction. The polymer blend systems investigated include (1) blends of polystyrene (PS) and poly(2,6-dimethylphenylene ether) (PPE),[3−5] (2) blends of poly(ethylene oxide) (PEO) and poly(methyl methacrylate) (PMMA),[6] (3) blends of PMMA and poly(styrene-*co*-acrylonitrile) (PSAN),[7−14] (4) blends of PMMA and poly(vinylidene fluoride) (PVDF),[9−11,15] (5) blends of PS and poly(vinyl methyl ether) (PVME),[16−28] (6) blends of PS and poly(α-methylstyrene) (PαMS),[22] (7) blends of polyisoprene (PI) and poly(vinylethylene) (PVE),[29−32] and (8) blends of 1,4-PI and 1,2-polybutadiene (PB).[33,34]

Table 1. Bond Energy and Relative Strength of Different Intermolecular Forces

type of interaction	bond energy (kJ/mol)	relative strength
ionic attraction	850−1700	1000
hydrogen bonding	50−170	100
dipole−dipole interaction	2−8	10
van der Waals interaction	∼1	1

It has been observed that some polymer blend systems without specific interaction exhibit a very broad, single glass transition.[18,22,30−33] A very broad, single glass transition has been observed when the difference in glass transition temperature (T_g) between the constituent components, ΔT_g, is large. Interestingly, it has been observed that time−temperature superposition (TTS) failed for miscible polymer blends without specific interaction when the polymer blends had large values of ΔT_g,[6,16,17,20−23,29−31,33−35] while an application of TTS to miscible polymer blends without specific interaction was warranted when they had small values of ΔT_g.[13,36,37] Strictly on an empirical basis, $\Delta T_g \approx 25$ °C has been found to be a reasonable value, below which an application of TTS to miscible polymer blends without specific interaction is valid.[13,37]

Understandably, the origin of very broad, single glass transition in miscible polymer blends without specific interaction has been the subject of an intensive investigation by many research groups for the past two decades. Today, it is a general consensus among researchers[17,21,29,33,38−45] that very broad, single glass transition in miscible polymer blends without

* To whom correspondence should be addressed. E-mail: cdhan@uakron.edu.

10.1021/ma7025385 CCC: $40.75
Published on Web 02/28/2008

specific interaction is caused by the presence of concentration fluctuations that broaden the distribution of segmental relaxation times, which depend not only on blend composition but also on temperature. Although some polymer blends are thermodynamically miscible, the component dynamics may be heterogeneous; namely, in such dynamically heterogeneous polymer blends, the components have measurably different segmental mobilities and relaxation times within the same composition. It then seems reasonable to speculate that a failure of TTS in miscible polymer blends without specific interaction may also be related to the presence of dynamic heterogeneity. Thus, much effort has been spent on a better understanding of segmental dynamics and dynamic heterogeneity in miscible polymer blends without specific interaction using different experimental methods including dielectric relaxation spectroscopy,[20,23] electron spin resonance spectroscopy,[42,46] solid-state nuclear magnetic resonance spectroscopy,[30,31,47−50] and the thermally stimulated depolarization current method.[51] It can then be concluded that concentration fluctuations, dynamic heterogeneity, failure of TTS, and the broadness of glass transition in miscible polymer blends without specific interaction are interrelated, as shown pictorially:

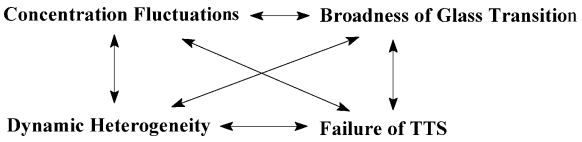

Today, it is well-established that hydrogen bonding enhances miscibility of a polymer blend.[52] During the past two decades, a number of research groups investigated the miscibility of polymer blends with specific interaction.[53−74] The polymer blend systems investigated include (1) blends of poly(vinylphenol) (PVPh) and PVME,[53−55] (2) blends of PVPh and poly(ethyl methacrylate) (PEMA),[56,57] (3) blends of PVPh and poly(vinyl acetate) (PVAc),[59,62] (4) blends of PVPh and poly(2-vinylpyridine) (P2VP),[69] and (5) blends of PVPh and poly(4-vinylpyridine) (P4VP).[70,71] However, to our surprise, to date only a few research groups[75,76] reported on the rheological behavior of miscible polymer blends with specific interaction. It is then fair to state that at present our understanding of the rheological behavior of miscible polymer blends with specific interaction is in an infant stage.

Very recently, we investigated linear dynamic viscoelasticity of four PVPh-based miscible polymer blend systems with specific interaction (intermolecular hydrogen bonding). The investigation was motivated to answer the fundamental question: How would the linear dynamic viscoelasticity of miscible polymer blends with intermolecular hydrogen bonding be different from that of miscible polymer blends without specific interaction? To answer the question posed above, we have attempted to answer the following specific questions. (1) Will an application of TTS to miscible polymer blends with intermolecular hydrogen bonding be warranted only when the difference in the component glass transition temperatures, ΔT_g, is smaller than a certain critical value, as has been found for miscible polymer blends without specific interaction? (2) Will concentration fluctuations and dynamic heterogeneity play significant roles in determining the rheological behavior of miscible polymer blends with intermolecular hydrogen bonding, as has been found for miscible polymer blends without specific interaction? In this paper we will summarize the highlights of our findings.

Table 2. Molecular Characteristics of the Five Homopolymers Employed in This Study

sample code	M_w	M_w/M_n
PVPh	2.16×10^4	1.62
PVAc	1.42×10^5	1.71
PVME	1.64×10^5	1.33
P2VP	4.11×10^4	1.37
P4VP	6.00×10^4	NA[a]

[a] P4VP was not soluble in common solvent, and thus it was not possible to determine M_w/M_n using solution GPC.

2. Experimental Section

Materials and Sample Preparation. In the present study we chose to prepare miscible blends of PVPh with PVME, poly(vinyl acetate) (PVAc), P2VP, and P4VP, for which PVPh, PVAc, and P4VP were purchased from Aldrich Chemical. Aqueous solution (50 wt %) of PVME was purchased from Scientific Polymer Products. After the water was removed completely, PVME was dissolved into toluene (5 wt % of solid) and precipitated using hexane. P2VP was synthesized by free radical polymerization. Table 2 give a summary of the molecular characteristics of the five homopolymers employed to prepare (1) PVPh/PVME blends, (2) PVPh/PVAc blends, (3) PVPh/P2VP blends, and (4) PVPh/P4VP blends.

Samples for rheological measurements and differential scanning calorimetry (DSC) experiments were prepared by solvent casting. Specifically, PVPh/PVME blends of different compositions were prepared by dissolving a predetermined amount of the constituent components in methyl ethyl ketone (5% solids in solution) in the presence of 0.1 wt % antioxidant (Irganox 1010, Ciba-Geigy Group), and then the solution was kept in a fume hood at room temperature for 24 h to allow for the evaporation of most of the solvent. Subsequently, the mixture was freeze-dried at room temperature for 3 days under vacuum and dried further at a temperature near its glass transition temperature (T_g) for 2 days under vacuum. A dried sample was compression-molded at T_g + 50 °C followed by annealing at T_g + 20 °C in a vacuum oven. A similar procedure was employed to prepare PVPh/PVAc blends using tetrahydrofuran (THF) as a solvent and PVPh/P2VP (or P4VP) blends using pyridine as a solvent.

Differential Scanning Calorimetry (DSC). The glass transition temperature (T_g) was determined by differential scanning calorimetry (DSC) (TA Instruments). DSC thermograms were recorded using a heating rate of 20 °C/min, and T_g is taken as the midpoint of the transition in the second scan.

Thermogravimetric Analysis (TGA). The thermal decomposition temperature was determined by thermogravimetric analysis (TGA) (TA Instruments) with a heating rate of 20 °C/min under a nitrogen atmosphere.

Fourier Transform Infrared (FTIR) Spectroscopy. Infrared spectra were recorded on a Fourier transform infrared (FTIR) spectrometer (Perkin-Elmer 16 PC FTIR), and 16 scans were collected with a spectral resolution of 4 cm^{-1}. The solution (2% w/v) containing the blend was cast onto potassium bromide (KBr) disk. The thickness of a film was adjusted, such that the maximum absorbance of any band was less than 1.0, at which the Beer−Lambert law is valid.

Rheological Measurements. Advanced Rheometric Expansion System (ARES) in the oscillatory mode with a parallel-plate fixture (8 mm diameter) was employed to measure the dynamic storage modulus (G') and dynamic loss modulus (G'') as functions of angular frequency (ω) ranging from 0.04 to 100 rad/s. For some samples, 0.005 rad/s was used as the lowest value of ω. Rheological measurements were taken at various temperatures ranging from T_g + 30 °C to T_g + 80 °C. All the measurements were conducted under a nitrogen atmosphere in order to avoid oxidative degradation of the samples. A single specimen was used for the entire rheological measurement, which took less than 3 h, at various temperatures below 200 °C, while a fresh specimen was used at each temperature above 200 °C.

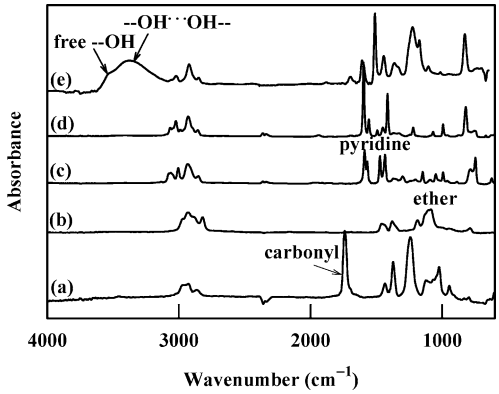

Figure 1. FTIR spectra for five neat polymers: (a) PVAc, (b) PVME, (c) P2VP, (d) P4VP, and (e) PVPh.

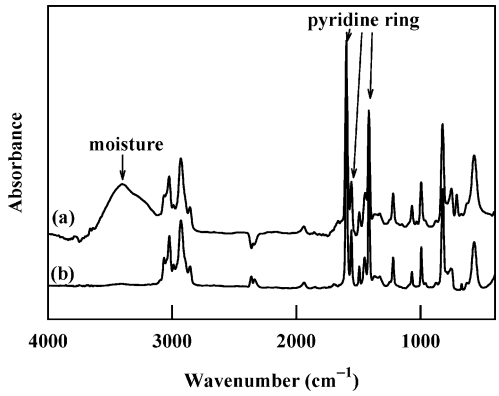

Figure 2. FTIR spectra for neat P4VP at room temperature: (a) before annealing; (b) held at 100 °C for 20 min followed by cooling to room temperature under a nitrogen atmosphere.

3. Results and Discussion

3.1. Self-Association and Rheological Behavior of Five Neat Homopolymers Investigated. FTIR spectroscopy has been proven to be a very powerful technique to detect the presence of self-association (intraassociation) within a given molecule (or polymer) or interassociation (intermolecular attractive interactions) between two chemically dissimilar molecules. For instance, the infrared (IR) hydroxyl stretching range of phenolic −OH group is sensitive to the formation of hydrogen bonds. Figure 1 gives FTIR spectra of the hydroxyl stretching vibration region for the five neat homopolymers employed in this study. In Figure 1 we observe two vibration bands in PVPh: one centered at 3530 cm^{-1} which is related to "free" hydroxyl group and another centered at 3380 cm^{-1} which is related to intraassociated hydrogen bonding of phenolic −OH group (i.e., self-association).[61] On the other hand, in Figure 1 we do not observe evidence of the presence of self-association in four other homopolymers, PVAc, PVME, P2VP, and P4VP. This observation is very important to interpret the rheological behavior of the four PVPh-based polymer blend systems investigated in this study, which is presented below. It should be mentioned at this juncture that TGA measurements of all five homopolymers indicate that thermal degradation temperature is higher than 320 °C, which is above the highest rheological measurements employed in this study.

It is known that P2VP and P4VP absorbs moisture very easily from air. Figure 2 gives FTIR spectra of P4VP before and after removing the moisture in the specimens, showing that the presence of an absorption band centered at 3300 cm^{-1} (the spectrum in Figure 2a) is due to the presence of moisture in the specimen. The FTIR spectrum of P4VP given in Figure 2b was obtained using a specimen that had been annealed at 100 °C under a nitrogen atmosphere for 20 min and then cooling to room temperature. As a result, the absorption band for moisture has disappeared completely in Figure 2b. We took the same precaution for all rheological experiments conducted in the present study. We mention this rather important observation made from this study for the reason that the rheological responses of P2VP and P4VP were found to be quite different after removal of moisture from the specimens.

Figure 3 gives plots of log G' vs log ω, log G'' vs log ω, and log G' vs log G'' at various temperatures for each of the four homopolymers, PVAc, PVME, P2VP, and P4VP. Notice in Figure 3 that the slope of log G' vs log G'' plots in the terminal region is very close to 2, and the plots are independent of temperature for all four homopolymers. Such an observation is a very clear rheological manifestation that all four homopolymers are homogeneous and free from self-association! It should be mentioned that we observed the slope of log G' vs log G'' plots in the terminal region for P2VP and P4VP to be smaller than 2 before moisture was removed from the specimens.

Figure 4 gives plots of log G' vs log ω, log G'' vs log ω, and log G' vs log G'' at various temperatures for PVPh after annealing at 200 °C for 1 h. It is of great interest to observe in Figure 4 that the slope of log G' vs log ω plots in the terminal region is much smaller than 2 at all four measurement temperatures, while the slope of log G'' vs log ω plots in the terminal region is very close to 1 at all four measurement temperatures. As a result, the slope of log G' vs log G'' plots in the terminal region for PVPh is much smaller than 2, which is quite different from the observation we have made above from Figure 3 for PVAc, PVME, P2VP, and P4VP. We wish to point out that the curvature of log G' vs log G'' plots in the terminal region for the PVPh has little to do with the sensitivity of transducer of ARES for the reason that the lowest value of G' (100 Pa) for PVPh given in Figure 4 is the same as that for PVAc, PVME, P2VP, and P4VP given in Figure 3, in which the slope of log G' vs log G'' plots in the terminal region is very close 2.

Earlier, Still and Whitehead[77] noted that a cross-linking reaction might occur for PVPh at elevated temperatures. Therefore, in obtaining the rheological data summarized in Figure 4, we investigated the extent of possible cross-linking reaction in PVPh at elevated temperatures by conducting solubility test of annealed PVPh specimens that had been subjected to various temperatures and durations in a vacuum oven, the results of which are summarized in Table 3. It can be seen in Table 3 that a PVPh specimen was soluble in THF after annealing at 200 °C for 3 h but partially insoluble after annealing at 200 °C for 24 h, and a PVPh specimen was soluble in THF after annealing at 220, 230, and 240 °C for 40 min but partially insoluble after annealing at 250 °C for 2 h. It should be mentioned that in all rheological measurements conducted in this study, including those summarized in Figures 3 and 4, all specimens had 0.1 wt % antioxidant (Irganox 1010, Ciba-Geigy Group). In the rheological measurements for PVPh, a single specimen was used at and below 200 °C under a nitrogen atmosphere. However, a fresh specimen was used at each temperature and each frequency sweep experiment that lasted less than 25 min. Therefore, we believe that the precaution taken in our rheological measurements precludes any possibility of cross-linking reaction in PVPh specimen. After each rheological measurement we confirmed that no cross-linking reaction took place in other homopolymers (PVAc, PVME, P2VP, and P4VP),

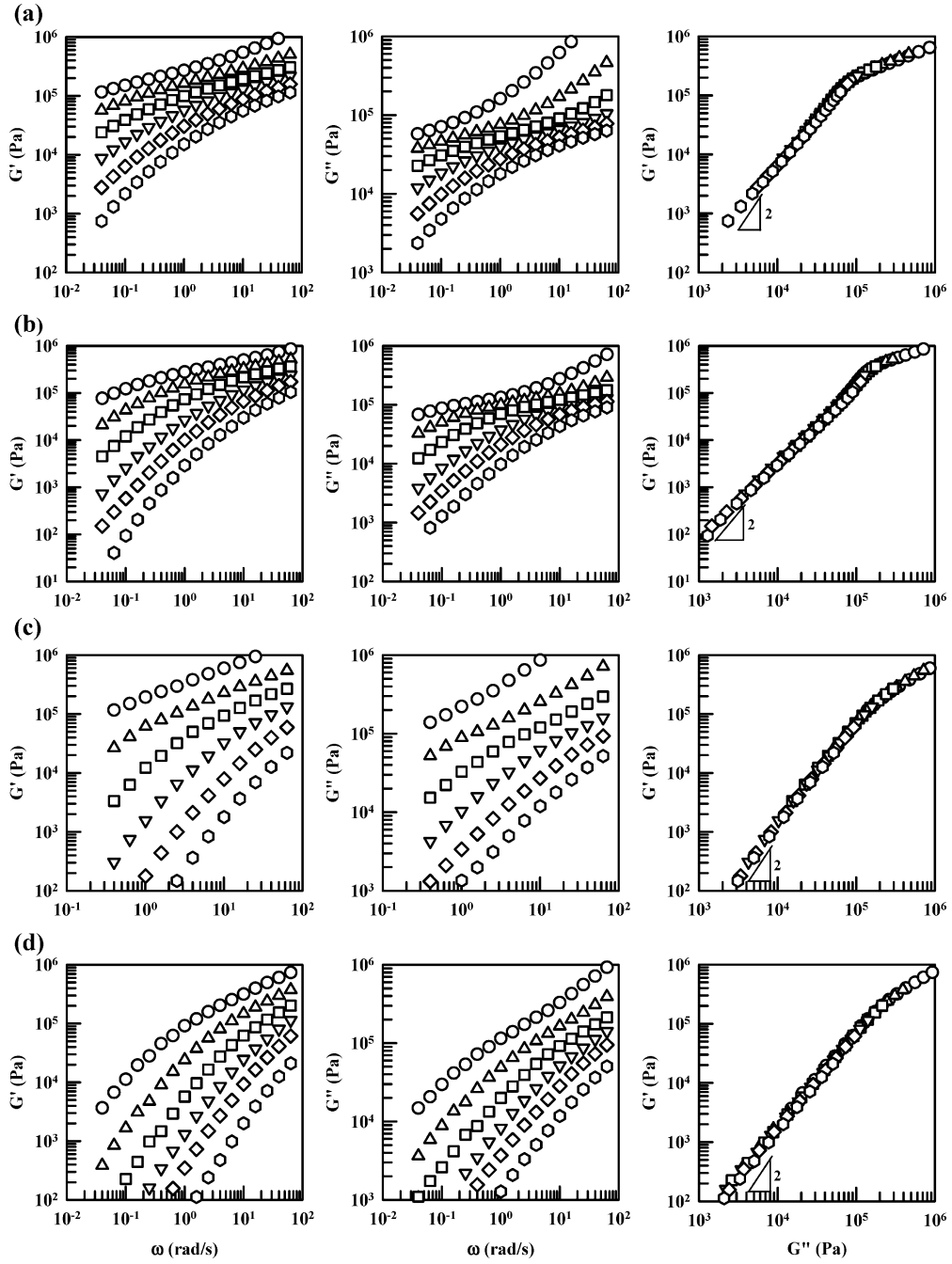

Figure 3. Rheology for four neat homopolymer: (a) PVAc at various temperatures (°C): (○) 58, (△) 68, (□) 78, (▽) 88, (◇) 98, and (⬡) 108; (b) PVME at various temperatures (°C): (○) 11, (△) 21, (□) 31, (▽) 41, (◇) 51, and (⬡) 61; (c) P2VP at various temperatures (°C): (○) 107, (△) 117, (□) 127, (▽) 137, (◇) 147, and (⬡) 157; (d) P4VP at various temperatures (°C): (○) 183, (△) 193, (□) 203, (▽) 213, (◇) 223, and (⬡) 233.

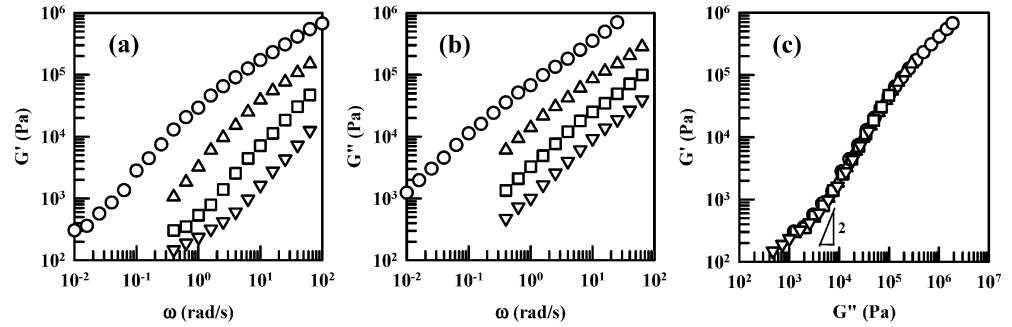

Figure 4. Rheology of neat PVPh at various temperatures (°C): (○) 200, (△) 210, (□) 220, and (▽) 230.

whose linear dynamic viscoelastic properties are summarized in Figure 3.

Zhang et al.[63] suggested that hydrogen bonding is a dynamic process, and hydrogen bonds are in equilibrium between

Table 3. Solubility of PVPh in THF after Annealing at Various Temperatures for Different Periods

annealing temperature (°C)	duration of annealing	solubility in THF
100	10 h	soluble
150	16 h	soluble
200	3 h	soluble
200	24 h	partially soluble
220	1 h	soluble
230	50 min	soluble
240	40 min	soluble
250	2 h	partially soluble

breaking and reassociating. If the lifetime of a hydrogen bond is longer than the segmental relaxation time, it is reasonable to speculate that PVPh might behave like a physically cross-linked network. Therefore, we attribute the curvature of log G' vs log G'' plots in the terminal region of PVPh, observed in Figure 4, to the presence of self-association in PVPh.

Before leaving this section, we wish to point out that, earlier, Han and co-workers[78,79] have shown that the log G' vs log G'' plot is dependent upon temperature, and its slope in the terminal region is smaller than 2 when a polymer has microdomains in block copolymers or thermoplastic polyurethanes and has a mesophase in liquid-crystalline polymers.

3.2. Strength of Specific Interaction, As Determined by FTIR Spectroscopy, in Four PVPh-Based Miscible Polymer Blend Systems. (a) Qualitative Analysis of Experimental Observations. Figure 5 gives FTIR spectra of the hydroxyl stretching vibration region for four PVPh-based blends. When the FTIR spectra of PVPh/PVME blends (see Figure 5a) are compared with the FTIR spectrum of neat PVPh, we observe that the absorption band of the hydrogen bonds between the phenolic −OH group in PVPh and the ether oxygen in PVME is shifted to a lower wavenumber, which is centered at about 3320 cm^{-1}. Zhang et al.[53] pointed out that the difference in wavenumber ($\Delta\nu_H$) between the absorption bands of hydrogen-bonded and free hydroxyl groups could be used as a measure of the relative strength of hydrogen bonding. According to them, the large value of $\Delta\nu_H$ ($\approx$210 cm^{-1}) in PVPh/PVME blends indicates that hydrogen bonding between PVME and PVPh is stronger than the self-association ($\Delta\nu_S$ = 150 cm^{-1}) among PVPh repeat units.

Referring to the FTIR spectra of PVPh/PVAc blends (see Figure 5b), the shoulder of the free hydroxyl group (3530 cm^{-1}) becomes undetectable, while the absorption band centered at 3380 cm^{-1} is shifted to a higher wavenumber (3458 cm^{-1}). This shift in wavenumber is attributable to the interassociation between PVPh and PVAc through hydrogen bonding. The difference in wavenumber between the interassociation due to hydrogen bonding in PVPh/PVAc blends and the free hydroxyl group is about $\Delta\nu_H$ = 72 cm^{-1} (a shift from 3530 to 3458 cm^{-1}), which is smaller than the shift in wavenumber ($\Delta\nu_S$ = 150 cm^{-1}) due to the self-association in PVPh. Therefore, the hydrogen bonding in PVPh/PVAc blends is weaker than that in neat PVPh.

Referring to the FTIR spectra of PVPh/P2VP blends (see Figure 5c), as the P2VP content in the blends increases, the intensity of the free hydroxyl band at a wavenumber of 3530 cm^{-1} decreases, indicating that more free hydroxyl groups in PVPh are hydrogen bonded with the pyridine groups in P2VP. Furthermore, the center of absorption band for the broad hydrogen bonding is shifted from 3380 to 3135 cm^{-1} when the content of P2VP increases to 60 wt %, yielding $\Delta\nu_H$ = 395 cm^{-1}. The large shift in wavenumber signifies a strong intermolecular hydrogen bonding between PVPh and P2VP.

The FTIR spectra of PVPh/P4VP blends (see Figure 5d) also exhibit the same trend as those of PVPh/P2VP blends. Since $\Delta\nu_H$ = 410 cm^{-1} in PVPh/P4VP blends, we can conclude that the strength of hydrogen bonds in PVPh/P4VP blends is slightly greater than that in PVPh/P2VP blends.[80]

From the above observations we conclude that the strength of the hydrogen bonds (SH) in the four PVPh-based miscible blends can be ranked as follows: $SH_{PVPh/P4VP}$ ($\Delta\nu_H$ = 410 cm^{-1}) > $SH_{PVPh/P2VP}$ ($\Delta\nu_H$ = 395 cm^{-1}) > $SH_{PVPh/PVME}$ ($\Delta\nu_H$ = 210 cm^{-1}) > $SH_{PVPh/PVAc}$ ($\Delta\nu_H$ = 72 cm^{-1}).

(b) Quantitative Analysis of Experimental Results via the Coleman−Graf−Painter (CGP) Association Model. The CGP association model[52] can be used to describe the thermodynamics of polymer blends with hydrogen bonding, which can be written using the following scheme:

$$B_1 + B_1 \rightleftharpoons B_2$$
$$B_h + B_1 \rightleftharpoons B_{h+1}$$

} Self-association

$$B_h + A_1 \rightleftharpoons B_hA_1 \qquad \text{Inter-association}$$

where B_1 represents phenolic −OH group, A_1 represents proton acceptors, such as ether, carbonyl, and pyridine group, B_2 is the hydrogen-bonded dimer formed between two phenolic −OH group, B_h is the hydrogen-bonded multimer, and B_hA_1 is the intermolecular hydrogen bonding.

The CGP association model for miscible polymer blends with hydrogen bonding can be summarized as follows[52]

$$\Phi_B = \Phi_{B_1}\left[\left(1 - \frac{K_2}{K_B}\right) + \frac{K_2}{K_B}\frac{1}{(1 - K_B\Phi_{B_1})^2}\right]\left[1 + \frac{K_A\Phi_{A_1}}{r}\right] \quad (1)$$

$$\Phi_A = \Phi_{A_1} + K_A\Phi_{A_1}\Phi_{B_1}\left[\left(1 - \frac{K_2}{K_B}\right) + \frac{K_2}{K_B}\frac{1}{1 - K_B\Phi_{B_1}}\right] \quad (2)$$

where Φ_B and Φ_A are the volume fractions of components B and A, respectively, in the blend, Φ_{B_1} and Φ_{A_1} are the volume fractions of free B and A groups, respectively, and $r = V_A/V_B$ with V_A and V_B respectively being the molar volumes of components A and B. K_2, K_B, and K_A appearing in eqs 1 and 2 are equilibrium constants, the definitions of which in terms of the hydrogen-bonded h-mer are given in the Supporting Information, corresponding to association, which can be determined from FTIR spectroscopic measurements of a dilute solution of low-molecular-weight analogue compounds (model compounds). For example, K_2 and K_B for PVPh were determined from the equilibrium constants for dilute solutions of phenol in cyclohexane.[81] Equations 1 and 2 give relationships between the composition (Φ_A and Φ_B) of a blend and the distribution of species present (Φ_{B_1} and Φ_{A_1}). The fraction of free B molecule (f_{FB}) can be determined from[52]

$$f_{FB} = \frac{\left(1 - \frac{K_2}{K_B}\right) + \frac{K_2}{K_B}\left(\frac{1}{(1 - K_B\Phi_{B_1})}\right)}{\left(1 - \frac{K_2}{K_B}\right) + \frac{K_2}{K_B}\left(\frac{1}{(1 - K_B\Phi_{B_1})^2}\right)}\left[\frac{1}{\left(1 + \frac{K_A\Phi_{A_1}}{r}\right)}\right] \quad (3)$$

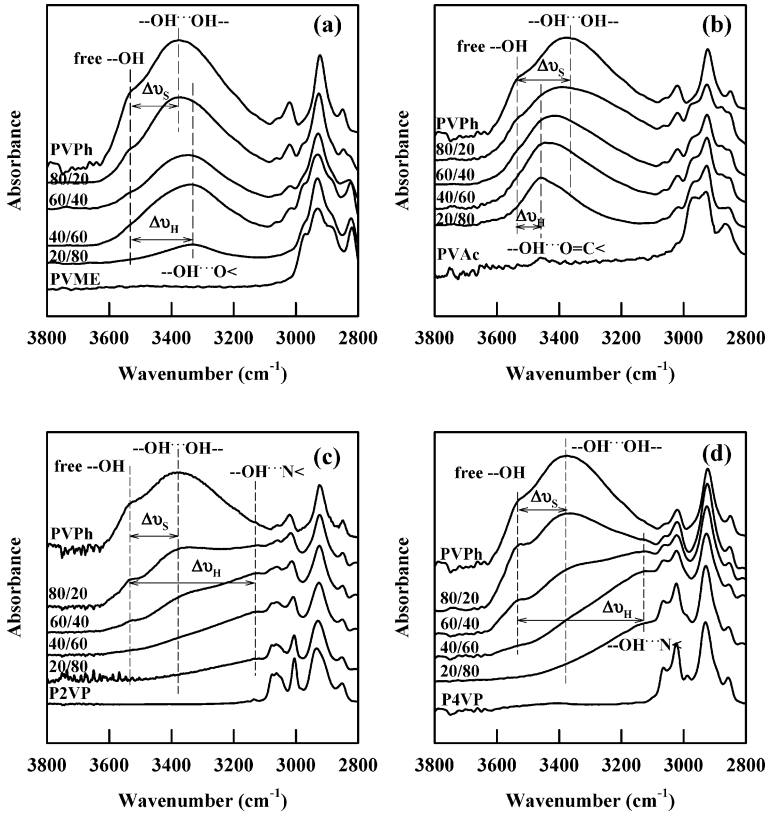

Figure 5. FTIR spectra at room temperature for (a) PVPh/PVME blends, (b) PVPh/PVAc blends, (c) PVPh/P2VP blends, and (d) PVPh/P4VP blends.

Table 4. Values of the Parameters Used for the Calculation of the Fraction of Hydrogen Bonding in Four PVPh-Based Blend Systems Investigated in This Study

					PVPh	
polymer	PVAc	PVME	P2VP	P4VP	hydrogen-bonded dimer	hydrogen-bonded multimer
V_A (mL/mol)	70.0	55.3	84.9	84.9	$V_B = 100.2$ (mL/mol)	
Δh_{BA} (cal/mol)	−4000	−5400	−5900	−6000	$\Delta h_2 = -5600$ (cal/mol)	$\Delta h_B = -5200$ (cal/mol)
K_A^o	57.5	88.3	500	598	$K_2^o = 21.0$	$K_B^o = 68.0$

and the fraction of hydrogen-bonded A groups (f_{BA}) can be determined from[52]

$$f_{BA} = 1 - f_{FA} = \left(1 - \frac{\Phi_{A_1}}{\Phi_A}\right) \tag{4}$$

The derivations of eqs 1−3 are given in the Supporting Information. The temperature dependence of equilibrium constants K_i can be expressed by

$$K_i = K_i^o \exp\left\{-\frac{\Delta h_i}{R}\left(\frac{1}{T} - \frac{1}{T^o}\right)\right\} \tag{5}$$

where K_i^o (i = 2, B, A) are the equilibrium constants at the absolute temperature T° (usually taken as 298 K), R is the universal gas constant, and Δh_i is the molar enthalpy of the formation of individual hydrogen bonds. Using eq 5, we can calculate the equilibrium constants (K_2, K_B, and K_A) at different temperatures. For example, for 20/80 PVPh/P4VP blend at 100 °C, we have $r = 0.849$, $\Phi_A = 0.8$, and $\Phi_B = 0.2$. From eq 5 we obtain $K_2 = 3.14$, $K_B = 11.65$, and $K_A = 78.10$.

For given blend compositions (Φ_B and Φ_A) and values of equilibrium constants (K_2, K_B, and K_A), we can calculate Φ_{B_1} and Φ_{A_1} from eqs 1 and 2. Then, substituting the calculated values of Φ_{B_1} and Φ_{A_1} into eqs 3 and 4, the quantities f_{FB} and f_{BA} can be calculated. The numerical values of the parameters necessary for the calculations of various quantities described above are summarized in Table 4, which are taken from the literature.[61,82,83] The values of the equilibrium constants and the molar enthalpy of the formation of hydrogen bonds in PVPh/P4VP blends reported in the literature are different depending on the sources.[84−87] In the present study we used the average values $\Delta h_{BA} = -6000$ cal/mol and $K_A = 598$ for PVPh/P4VP blends, and we used $K_A = 500$ for PVPh/P2VP blends.[88] We estimated the value of the molar enthalpy of the formation of hydrogen bonds in PVPh/P2VP blends to be $\Delta h_{BA} = -5900$

Table 5. Calculated Fractions of Free Hydrogen Group B and Hydrogen-Bonded Group A for Four PVPh-Based Blend Systems Investigated in This Study

composition (wt %)	20/80	40/60	60/40	80/20
	PVPh/ PVAc blends			
f_{FB}	0.062	0.089	0.116	0.143
f_{BA}	0.156	0.345	0.507	0.628
	PVPh/PVME blends			
f_{FB}	0.051	0.073	0.101	0.132
f_{BA}	0.126	0.293	0.462	0.599
	PVPh/P2VP blends			
f_{FB}	0.019	0.039	0.090	0.134
f_{BA}	0.202	0.506	0.785	0.879
	PVPh/P4VP blends			
f_{FB}	0.016	0.034	0.087	0.134
f_{BA}	0.207	0.517	0.803	0.893

Table 6. Summary of the Thermal Properties of Four PVPh−Based Blend Systems Investigated in This Study

	PVPh/PVAc		PVPh/PVME		PVPh/P2VP		PVPh/P4VP	
PVPh content (wt %)	T_{gm} (°C)	Δw_{T_g} (°C)	T_{gm} (°C)	Δw_{T_g} (°C)	T_{gm} (°C)	Δw_{T_g} (°C)	T_{gm} (°C)	Δw_{T_g} (°C)
0	28	10	−19	9	97	11	153	11
20	44	19	−1	28	121	21	179	20
40	65	20	24	24	146	19	186	21
60	101	28	72	21	161	17	192	20
80	140	17	106	18	171	16	186	25
100	180	10	180	10	180	10	180	10

cal/mol (because the specific interaction in PVPh/P2VP blends is slightly weaker than that in PVPh/P4VP blends). The calculated values of the fraction of free B groups and hydrogen-bonded A groups are summarized in Table 5. It can be seen from Table 5 that both f_{FB} and f_{BA} increase as the amount of PVPh in the respective blend systems increases. A close examination of the values of f_{BA} given in Table 5 reveals that the stronger the specific interactions, the larger the values of f_{BA}, i.e., the more intermolecular hydrogen bonds have been formed. For example, at the same composition, f_{BA} of PVPh/P4VP blends are much larger than f_{BA} of PVPh/PVAc blends. The procedures used to calculate the fraction of the hydrogen bonds formed for the four PVPh-based miscible polymer blends are described in the Supporting Information.

3.3. Strength of Hydrogen Bonds, As Determined by DSC, in Four PVPh-Based Miscible Polymer Blend Systems. The glass transition of all four PVPh-based blend systems has been studied using DSC. Figure 6 gives DSC thermograms of four different blend compositions for each blend system investigated. A broad, single glass transition for each blend composition is observed in Figure 6, in which the arrow upward denotes the onset point (T_{gi}), the symbol + denotes the midpoint (T_{gm}), and the arrow downward denotes the end point (T_{gf}) of the glass transition. A single T_g, though broad, indicates that each blend is miscible within the size scale which DSC can detect and each of the four blend systems investigated is miscible over the entire blend composition. Table 6 gives a summary of the glass transition temperature (T_g) in terms of T_{gm} and the width of glass transition temperature denoted by $\Delta w_{T_g} = T_{gf} - T_{gi}$ for each blend composition of all four PVPh-based blend systems investigated in this study. It is seen in Table 6 that the Δw_{T_g} for a certain blend composition is as large as 28 °C, while the Δw_{T_g} for neat components is about 10 °C. Notice in Table 6 that the difference in T_{gm} between the constituent components, ΔT_{gm}, is 152 °C for PVPh/PVAc blends, 199 °C for PVPh/PVME blends, 83 °C for PVPh/P2VP, and 27 °C for PVPh/P4VP blends. It should be mentioned at this juncture that earlier Kim et al.[22] investigated the thermal transition behavior of miscible PS/PVME and PS/PαMS blend systems that have no specific interactions. They reported that Δw_{T_g} was as large as 42 °C for a certain blend composition of PS/PVME blends and as large as 58 °C for a certain blend composition of PS/PαMS blends, while ΔT_{gm} between the constituent components was about 120 °C for PS/PVME blends and about 75 °C for PS/PαMS blends.

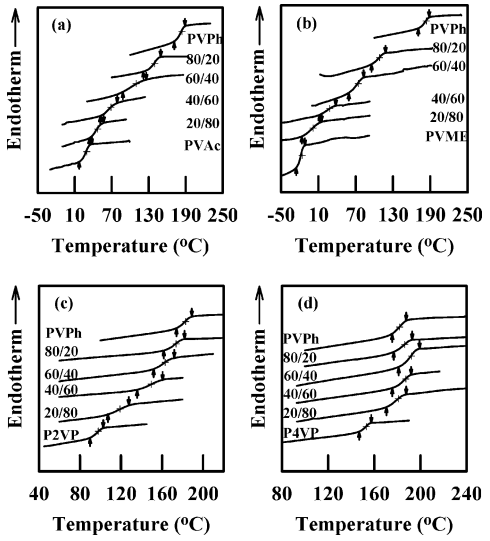

Figure 6. DSC thermograms for (a) PVPh/PVAc blends, (b) PVPh/PVME blends, (c) PVPh/P2VP blends, and (d) PVPh/P4VP blends.

It is of great interest to note from the above observations that values of Δw_{T_g} for PVPh/PVAc and PVPh/PVME blends are much smaller than those of PS/PVME and PS/PαMS blends, in spite of the fact that values of ΔT_{gm} for PVPh/PVAc and PVPh/PPVME blends are much larger than those for PS/PVME and PS/PαMS blends. In other words, the magnitude of ΔT_{gm} between the constituent components in the PVPh-based blend systems with hydrogen bonding does not seem to be correlated to the magnitude of Δw_{T_g}. The above observations lead us to conclude that the PVPh-based blend systems with hydrogen bonding have smaller values of Δw_{T_g} than the PS/PVME and PS/PαMS blend systems without specific interaction reported by Kim et al.[22] As summarized in the Introduction, the current consensus, though strictly empirical, among researchers is that the broadness of glass transition is related to the extent of composition fluctuations and dynamic heterogeneity in miscible polymer blends without specific interaction, and a failure of TTS in such blend systems is associated with the presence of concentration fluctuations and dynamic heterogeneity. What remains to be seen here is whether such a consensus would also be applicable to the PVPh-based blend systems with

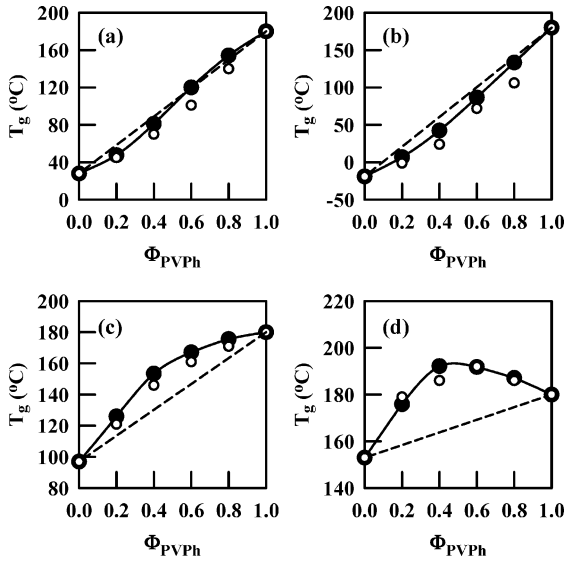

Figure 7. Composition-dependent glass transition temperatures (T_g) for (a) PVPh/PVAc blends, (b) PVPh/PVME blends, (c) PVPh/P2VP blends, and (d) PVPh/P4VP blends, in which the dashed line represents a linear behavior, the open symbols (○) denote experimental data, and the filled symbols (●) denoted predicted values from eq 6.

Table 7. Parameters Used To Predict the Composition Dependence of T_{gm} for Four PVPh-Based Blend Systems Investigated in This Study

polymer	PVAc	PVME	P2VP	P4VP	PVPh
M_A	86.1	58.1	105.2	105.2	$M_B = 120.2$
T_{gA} (°C)[a]	28	−19	97	153	$T_{gB} = 180$ °C
ΔC_{pA} (cal/(g K))[b]	0.108	0.142	0.156	0.156	$\Delta C_{pB} = 0.128$ cal/(g K)

[a] Experimental data. [b] Obtained by the heat capacity group contribution method.[98]

hydrogen bonding. If it does, we will be able to conclude that TTS would work for the PVPh-based blend systems owing to a lesser degree of, if not negligible, concentration fluctuations and dynamic heterogeneity.

Plots of experimentally determined T_g (accurately stated, T_{gm}) vs blend composition (open symbols) for four PVPh-based blend systems are given in Figure 7, in which the dashed lines represent a linear relationship and the solid lines are drawn through the filled symbols that were obtained from calculations using the theory presented below. Numerical values of the experimentally determined T_{gm} are given in Table 6. It is seen in Figure 7 that both PVPh/PVAc and PVPh/PVME blend systems show negative deviation from a linear relationship, while both PVPh/P2VP and PVPh/P4VP blend systems show positive deviation from a linear relationship.

In the past, several research groups[83,89−97] suggested expressions for relationships between T_g and blend compositions in miscible polymer blend systems; some expressions are for miscible polymer blend systems without specific interaction,[89−93] and others are for miscible polymer blend systems with specific interactions.[83,94−97] The majority of the suggested expressions for miscible polymer blend systems with specific interactions, with an exception for the thermodynamic theory of Painter et at.,[83] have at least one adjustable parameter. The most comprehensive theory predicting the composition dependence of glass transition temperature of miscible polymer blends with specific interactions is given by Painter et al.,[83] according to which we have the following expression:

$$T_{gm} = \frac{X_A T_{gA} + K_0 X_B T_{gB}}{X_A + K_0 X_B} + q X_A X_B \qquad (6)$$

in which T_{gm} is the midpoint of glass transition temperature, as determined from a DSC thermogram (see Figure 6), X_A and X_B are the mole fractions of components A and B, respectively, with the subscript B referring to the self-associating component (PVPh in the present study), T_{gA} and T_{gB} are the glass transition temperatures of components A and B, respectively, and K_0 is the ratio of heat capacity ($K_0 = \Delta C_{pB}/\Delta C_{pA}$) with ΔC_{pB} and ΔC_{pA} being the heat capacities of components A and B, respectively, and q is defined by

$$q = -\frac{X_B\{[H_B^{H,1}]_{T_{gm}} - [H_B^{H,1}]_{T_{gB}}\} + \Delta H_m^{H,1}}{X_A X_B (X_A + K_0 X_B)\Delta C_{pA}}$$

$$= -\frac{X_B n_B \Delta h_B\{[p^{\circ}_{BB}]T_{gm} - [p^{\circ}_{BB}]T_{gB}\} + n_B \Delta h_B[p_{BB} - p^{\circ}_{BB}]T_{gm} + n_A \Delta h_{BA}[P_{BA}]T_{gm}}{X_A X_B (X_A + K_0 X_B)\Delta C_{pA}} \qquad (7)$$

The definitions and the physical meanings of the various parameters ($H_B^{H,1}$, $\Delta H_m^{H,1}$, n_A, n_B, Δh_B, Δh_{BA}, p_{BB}, p_{BA}, and p°_{BB}) appearing in eq 7 are given in the Supporting Information. Equation 6 predicts both positive and negative deviations from the linear mixing rule. For $q = 0$, eq 6 reduces to the well-known Gordon−Taylor equation.[89] For the derivation of eq 7, the readers are referred to the original paper.[83] Table 7 gives numerical values of the parameters (M_A, T_{gA}, and ΔC_{pA}) for PVAc, PVME, P2VP, P4VP, and PVPh that are needed to predict the composition dependence of T_{gm} using eq 6 with the aid of eq 7.

Table 8. Values of Three Terms on the Right-Hand Side of Eq 7 for Four PVPh-Based Blend Systems Investigated in This Study

	$-X_B n_B \Delta h_B\{[p^{\circ}_{BB}]_{T_{gm}} - [p^{\circ}_{BB}]_{T_{gB}}\}$	$-n_B \Delta h_B[p_{BB} - p^{\circ}_{BB}]_{T_{gm}}$	$-n_A \Delta h_{BA}\cdot[p_{BA}]_{T_{gm}}$
PVPh/PVAc			
20/80	0.22	−6.35	5.31
40/60	0.74	−8.54	7.52
60/40	1.13	−7.00	6.69
80/20	0.97	−3.79	3.92
PVPh/PVME			
20/80	0.19	−7.28	7.98
40/60	0.73	−10.58	12.14
60/40	1.38	−8.50	10.78
80/20	1.53	−4.27	6.17
PVPh/P2VP			
20/80	0.12	−6.73	9.08
40/60	0.25	−10.62	14.68
60/40	0.28	−8.60	12.11
80/20	0.18	−4.18	6.28
PVPh/P4VP			
20/80	0.01	−6.14	8.97
40/60	−0.12	−9.95	14.52
60/40	−0.27	−8.68	12.42
80/20	−0.30	−4.25	6.43

Earlier, Kwei[94] proposed an expression that has the same form as eq 6, but K_0 and q in the Kwei expression are adjustable parameters. Kwei then suggested that the empirical parameter q in his expression describes the strength of specific interactions with positive values representing strong specific interactions between the constituent components and negative values representing weak specific interactions between the constituent components.

On the other hand, values of composition-dependent q defined by eq 7 can be calculated accurately with the information on the various quantities appearing in the expression; i.e., there are no adjustable parameters in eqs 6 and 7. Let us consider the four PVPh-based miscible blend systems investigated in this study. Notice that the numerator on the right-hand side of eq 7 consists of three terms. The first term ($-X_B n_B \Delta h_B\{[p^{\circ}_{BB}]_{T_{gm}} - [p^{\circ}_{BB}]_{T_{gB}}\}$) describes the difference in self-association of PVPh between two different temperatures, one at the midpoint of blend glass transition temperature T_{gm} and another at the glass transition temperature of neat PVPh T_{gB}; i.e., this term represents the effect of temperature on self-association. The second term ($-n_B \Delta h_B[p_{BB} - p^{\circ}_{BB}]_{T_{gm}}$) describes the difference in self-association of PVPh between two situations, one after mixing and another before mixing; i.e., this terms represents the effect of mixing on self-association of PVPh. The third term ($-n_A \Delta h_{BA}[p_{BA}]_{T_{gm}}$) describes the interassociation (intermolecular attractive interactions) between the constituent components at T_{gm}. Using the numerical values of the parameters listed in Tables 4 and 7, we calculated values of the three terms appearing on the right-hand side of eq 7 for the four PVPh-based blend systems, and they are given in Table 8.

The following observations are worth noting in Table 8. (1) The magnitude of the first term on the right-hand side of eq 7

Table 9. Values of *q* Calculated from Eq 7 for Four PVPh-Based Blend Systems Investigated in This Study

composition (wt %)	PVPh/PVAc blends	PVPh/PVME blends	PVPh/P2VP blends	PVPh/P4VP blends
20/80	−57.43	65.63	111.35	127.78
40/60	−10.97	90.04	127.16	131.15
60/40	27.60	110.34	110.24	100.89
80/20	46.86	115.06	98.46	81.17

is much smaller than that of the other terms, indicating that the effect of temperature on self-association makes rather small contributions to the overall values of q defined by eq 7. (2) For the PVPh/PVAc blend system, the magnitude of the second term on the right-hand side of eq 7 is comparable with or slightly larger than that of the third term, the two terms having opposite signs. This observation suggests that values of q (i.e., the sum of the three terms in eq 7) can be even negative for the blends having less than say about 50 wt % of PVPh in PVPh/PVAc blends, indicating that the self-association of phenolic −OH group in the blends would be predominant over the intermolecular attractive interactions between the constituent components. Under such circumstances, q defined by eq 7 does not reflect the strength of intermolecular attractive interactions in miscible PVPh/PVAc blends. (3) For low concentrations of PVPh in the PVPh/PVME blend system, the magnitude of the third term, having a positive sign, on the right-hand side of eq 7 are slightly larger than that of the second term having a negative sign, and the magnitude of the third term becomes larger with increasing concentration of PVPh. This observation indicates that intermolecular attractive interactions between the constituent components in PVPh/PVME blends become predominant over self-association of PVPh in the blends. (4) For the PVPh/P2VP and PVPh/P4VP blend systems, the magnitude of the third term, having a positive sign, on the right-hand side of eq 7 is conspicuously larger than that of the second term, having a negative sign, over the entire blend composition. This observation indicates that the intermolecular attractive interactions between the constituent components are predominant over the self-association of PVPh in the PVPh/P2VP and PVPh/P4VP blend systems.

Table 9 gives a summary of the values of q defined by eq 7 as a function of composition for all four PVPh-based miscible blend systems investigated. Note in Table 9 that the sign of q can be positive or negative, depending on the sign and the magnitude of the three terms appearing on the right-hand side of eq 7 (see Table 8). For low concentrations of PVPh (e.g., 20 wt %), since PVPh is surrounded by large amounts of non-self-associating component, the effect of self-association of PVPh on the values of q would be small. In this situation, the value of q reflects the contribution of interassociation and then a large positive value of q indicates strong intermolecular attractive interactions in a miscible polymer blend. It can be seen clearly from Table 9 that 20/80 PVPh/ P4VP blend has a large positive value of q, while 20/80 PVPh/PVAc has a negative value of q. Therefore, we can rank the strength of attractive interactions (SA) in the following order: $SA_{PVPh/P4VP} > SA_{PVPh/P2VP} > SA_{PVPh/PVME} > SA_{PVPh/PVAc}$. This observation is consistent with that made from the FTIR spectra given in Figure 5.

We predicted, via eq 6, composition-dependent T_{gm}, and they are summarized in Figure 7 (filled symbols), in which the dashed line represents a linear relationship and the solid line is drawn through the predicted values to guide the eyes. It can be seen from Figure 7 that the predicted composition dependence of T_{gm} for the four PVPh-based miscible polymer blend systems is in good agreement with experimental results. The details of the procedures employed to calculate T_{gm} are given in the Supporting Information.

What is of great interest in Figure 7 is that, among the four PVPh-based blend systems investigated, PVPh/P4VP and PVPh/P2VP blend systems have positive deviation from linearity, while PVPh/PVAc and PVPh/PVME blend systems have slightly negative deviation from linearity. Notice that the PVPh/P4VP blend system has a larger deviation from linearity as compared with the PVPh/P2VP blend system.

3.4. Linear Dynamic Viscoelasticity of Four PVPh-Based Miscible Polymer Blend Systems Investigated. (a) Construction of Reduced Plots of Dynamic Moduli, Composition Fluctuations, and Time−Temperature Superposition. Figure 8 gives plots of log G' vs log ω and log G'' vs log ω for 20/80 PVPh/PVME blend at various temperatures ranging from 29 to 79 °C. Similar plots were obtained for other blend compositions, but they are not presented here owing to the limited space available. It is seen in Figure 8 that both G' and G'' decrease with increasing temperature. To obtain temperature-independent generalized (reduced) plots for the dynamic loss modulus G'', log G'' vs log ω plots given in Figure 8 were shifted along the ω axis to overlap the log G'' vs log ω plots at a reference temperature $T_r = T_{gm} + 50$ °C, with T_{gm} being the midpoint of

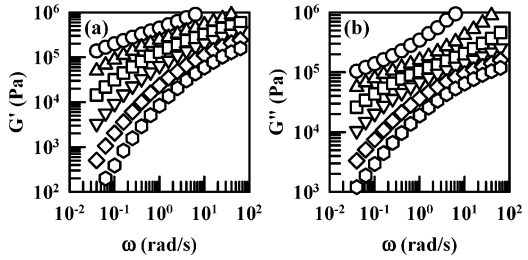

Figure 8. (a) Log G' vs log ω plots and (b) log G'' vs log ω plots for 20/80 PVPh/PVME blend at various different temperatures (°C): (○) 29, (△) 39, (□) 49, (▽) 59, (◇) 69, and (⬡) 79.

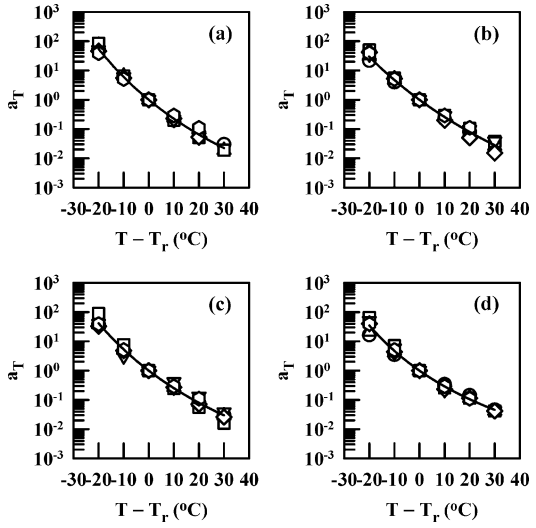

Figure 9. Plots of a_T vs $T - T_r$ with $T_r = T_{gm} + 50$ °C as the reference temperature for (a) PVPh/PVAc blends, (b) PVPh/PVME blends, (c) PVPh/P2VP blends, and (d) PVPh/P4VP blends at various blend compositions: (○) 0/100, (△) 20/80, (□) 40/60, (▽) 60/40, (◇) 80/20, and (⬡) 100/0. The solid line represents a fit to the WLF expression.

Table 10. WLF Constants for Four PVPh-Based Blend Systems Investigated in This Study

blends	C_1	C_2 (°C)
PVPh/PVAc blends	7.74	105.88
PVPh/PVME blends	8.81	140.23
PVPh/P2VP blends	6.76	101.59
PVPh/P4VP blends	5.14	86.49

glass transition temperature of 20/80 PVPh/PVME blend, in which 20/80 refers to the weight percent of the constituent components. The amount of shift made along the ω axis, which is temperature dependent, is commonly referred to as shift factor a_T.

Figure 9 gives plots of log a_T vs $T - T_r$ with $T_r = T_{gm} + 50$ °C for the four PVPh-based miscible polymer blend systems, in which symbols represent values of a_T that were obtained by shifting log G'' vs log ω plots along the ω axis with $T_r = T_{gm} + 50$ °C for each blend. The solid lines in Figure 9 are theoretical predictions from the WLF expression[99]

$$\log a_T = \frac{-C_1(T - T_r)}{C_2 + (T - T_r)} \tag{8}$$

In obtaining the solid lines in Figure 9, the constants C_1 and C_2 in eq 8 were determined by fitting the experimentally determined a_T to eq 8, and the values of the WLF constants determined for each blend system are summarized in Table 10. It is seen from Figure 9 that plots of log a_T vs $T - T_r$ are independent of blend composition for each blend system, indicating that an iso-free volume state is warranted for each blend system.

Log G' vs log $a_T\omega$ and log G'' vs log $a_T\omega$ plots are given in Figure 10a for 20/80 PVPh/PVME blend and in Figure 10b for 60/40 PVPh/PVME blend at various temperatures with $T_r = T_g + 50$ °C, for which values of a_T given in Figure 9 were used. Similar plots for other blend ratios are not presented here for the reason of limited space available. In Figure 10a,b we have temperature-independent log G' vs log $a_T\omega$ plots with a slope less than 2 in the terminal region for both 20/80 and 60/40 PVPh/PVME blends. Before making a general statement, let us observe further whether the log G' vs log $a_T\omega$ plots for three other PVPh-based miscible blend systems investigated would also show the same trend as those for PVPh/PVME blends. Log G' vs log $a_T\omega$ and log G'' vs log $a_T\omega$ plots are given in Figure 10c for 20/80 PVPh/PVAc blend and in Figure 10d for 60/40 PVPh/PVAc blend at various temperatures with $T_r = T_{gm} + 50$ °C.

Log G' vs log $a_T\omega$ and log G'' vs log $a_T\omega$ plots are given in Figure 10e for 20/80 PVPh/P2VP blend and in Figure 10f for 60/40 PVPh/P2VP blend at various temperatures with $T_r = T_{gm} + 50$ °C. Log G' vs log $a_T\omega$ and log G'' vs log $a_T\omega$ plots are given in Figure 10g for 20/80 VPh/P4VP blend and Figure 10h for 60/40 PVPh/P4VP blend at various temperatures with $T_r = T_{gm} + 50$ °C. It is clearly seen in Figure 10a−h that the log G' vs log $a_T\omega$ plots for all four PVPh-based miscible blend systems show temperature independence, indicating that TTS works. After each rheological measurement we confirmed that no cross-linking reaction took place in all four PVPh-based miscible polymer blends, whose linear dynamic viscoelastic properties are summarized in Figure 10.

Earlier, Ajii et al.[16,17] and Kapnistos[21] reported that the log G' vs log $a_T\omega$ plots in the terminal region of miscible PS/PVME blends without specific interaction varied with temperature and had a curvature in the terminal region. The authors concluded that TTS failed for the PS/PVME blends because log G' vs log $a_T\omega$ plots varied with temperature. Notice that there is a clear difference in the temperature dependence of log G' vs log $a_T\omega$ plots between the miscible PVPh/PVME blend system with hydrogen bonding investigated in this study and the miscible PS/PVME blend system without specific interaction reported by Ajii et al.[16,17] and Kapnistos.[21] Yang et al.[11] observed that the log a_T vs T plots were independent of blend composition for PMMA/PSAN blends but dependent upon blend composition for PMMA/PVDF blends. They further observed that TTS worked very well for PMMA/PSAN blends while TTS failed for PMMA/PVDF blends. One of the differences between PMMA/PSAN blends and PMMA/PVDF blends is that the difference in T_g, ΔT_g, between the constituent components of PMMA/PSAN blends is relatively small (≈20 °C) while PVDF in PMMA/PVDF blends is a semicrystalline polymer. According

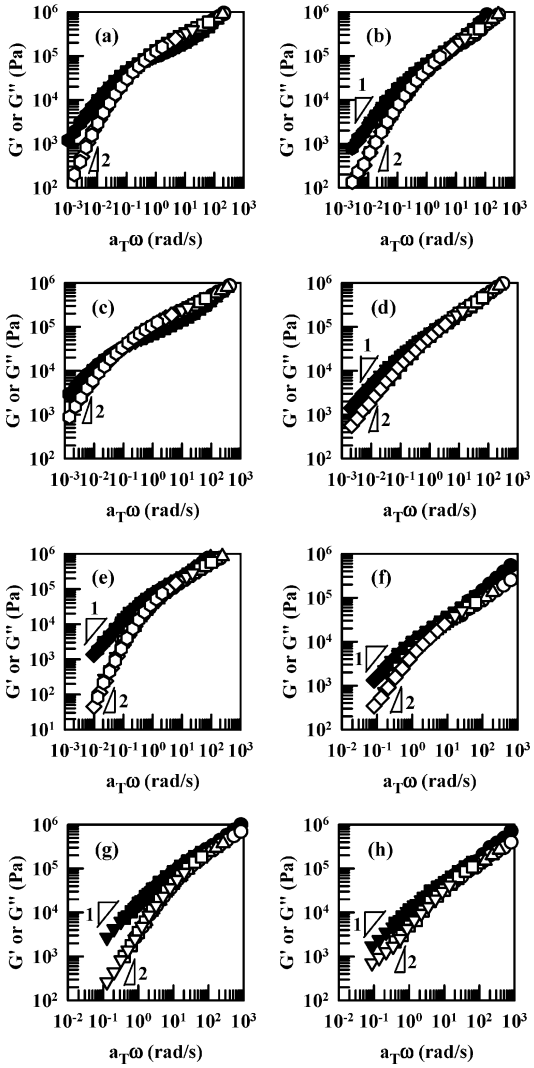

Figure 10. Plots of log G' vs log $a_T\omega$ (open symbols) and log G'' vs log $a_T\omega$ (filled symbols) with $T_r = T_{gm} + 50$ °C as the reference temperature for: (a) 20/80 PVPh/PVME blend at various temperatures (°C): (○, ●) 29, (△, ▲) 39, (□, ■) 49, (▽, ▼) 59, (◇, ◆) 69, and (⬡, ⬢) 79; (b) 60/40 PVPh/PVME blend at various temperatures (°C): (○, ●) 102, (△, ▲) 122, (□, ■) 132, (▽, ▼) 142, (◇, ◆) 152, and (⬡, ⬢) 162; (c) 20/80 PVPh/PVAc blend at various temperatures (°C): (○, ●) 74, (△, ▲) 84, (□, ■) 94, (▽, ▼) 104, (◇, ◆) 114, and (⬡, ⬢) 124; (d) 60/40 PVPh/PVAc blend at various temperatures (°C): (○, ●)131, (△, ▲) 141, (□, ■) 151, (▽, ▼) 161, and (◇, ◆) 171; (e) 20/80 PVPh/P2VP blend at various temperatures (°C): (○, ●) 151, (△, ▲) 161, (□, ■) 171, (▽, ▼) 181, (◇, ◆) 191, and (⬡, ⬢) 201; (f) 60/40 PVPh/P2VP blend at various temperatures (°C): (○, ●) 191, (△, ▲) 201, (□, ■) 211, (▽, ▼) 221, and (◇, ◆) 231; (g) 20/80 PVPh/P4VP blend at various temperatures (°C): (○, ●) 209, (△, ▲) 219, (□, ■) 229, and (▽, ▼) 239; (h) 60/40 PVPh/P4VP blend at various temperatures (°C): (○, ●) 222, (△, ▲) 232, (□, ■) 242, and (▽, ▼) 252.

to the observations made by Pathak et al.[13] and Friedrich et al.,[37] TTS would work for miscible polymer blends without specific interaction when ΔT_g is about 25 °C or less. However, the same empirical criterion does not seem applicable to the four PVPh-based miscible blend systems investigated in this study because $\Delta T_g = 152$ °C for PVPh/PVAc blends, $\Delta T_g = 199$ °C for PVPh/PVME blends, $\Delta T_g = 83$ °C for PVPh/P2VP blends, and $\Delta T_g = 27$ °C for PVPh/P2VP blends. That is, in spite of the large differences in ΔT_g among the four PVPh-based miscible blend systems, log a_T vs $T - T_r$ plots are independent of blend composition (see Figure 9) and log G' vs log $a_T\omega$ plots in the terminal region are independent of temperature for all four PVPh-based miscible blend systems (see Figure 10). If we maintain the view that a failure of TTS in miscible polymer blends without specific interaction (e.g., PEO/PMMA blends; PS/PVME; PS/PαMS blends; PI/PVE blends) is associated with the presence of concentration fluctuations and dynamic heterogeneity, we are then led to conclude that the extent of concentration fluctuations and dynamic heterogeneity in the four PVPh-based miscible blend systems with hydrogen bonding might be very small, if not negligible, because TTS works.

Notice in Figure 10a−h for the PVPh-based miscible blends that the log G' vs log $a_T\omega$ plots are independent of temperature over the entire range of temperatures investigated, and their slopes in the terminal region are less than 2 while maintaining temperature independence. We attribute this observation to the presence of hydrogen bonding in each of the PVPh-based miscible polymer blends investigated. The origin of this observation is quite different from that reported by Ajii et al.[16,17] and Kapnistos,[21] who observed temperature dependence of log G' vs log $a_T\omega$ plots for miscible PS/PVME blends without specific interaction, which then led them to conclude that TTS failed for the PS/PVME blends. Further, in their studies the log G' vs log $a_T\omega$ plots in the terminal region had conspicuous irregularity in the temperature dependence. Thus, there is no similarity in the origin of the terminal region behavior of log G' vs log $a_T\omega$ plots observed between the two studies.

Owing to the limited space available, in Figure 10, we combined eight plots in a single figure. In doing so, we had to use small-size plots for each blend. In order to observe whether the small-size plots might have obscured the quality of the correlation obtained, we have prepared enlarged plots of log G' vs log $a_T\omega$ and log G'' vs log $a_T\omega$ for 60/40 PVPh/PVME and 60/40 PVPh/P2VP blends at various temperatures. They are designated as Figures S4 and S5 and are given in the Supporting Information. We have found little difference in the quality of reduced plots between Figure 10 and the enlarged plots (Figures S4 and S5) given in the Supporting Information, leading us to conclude that application of TTS is warranted for the four PVPh-based miscible polymer blend systems investigated in this study. Further, in order to observe whether plots of loss angle against reduced angular frequency might be very sensitive to shifting, we also prepared log tan δ vs log $a_T\omega$ plots, together with log G' vs log $a_T\omega$ and log G'' vs log $a_T\omega$ plots, for PVPh/PVAc, PVPh/ PVME, PVPh/P2VP, and PVPh/P4VP blends. They are designated as Figures S6, S7, S8, and S9 and are given in the Supporting Information. We have found little difference in the sensitivity to shifting between log tan δ vs log $a_T\omega$ plot and log G' vs log $a_T\omega$ plot, and between log tan δ vs log $a_T\omega$ plot and log G'' vs log $a_T\omega$ plot, leading us to conclude that application of TTS is warranted for the four PVPh-based miscible polymer blend systems investigated in this study.

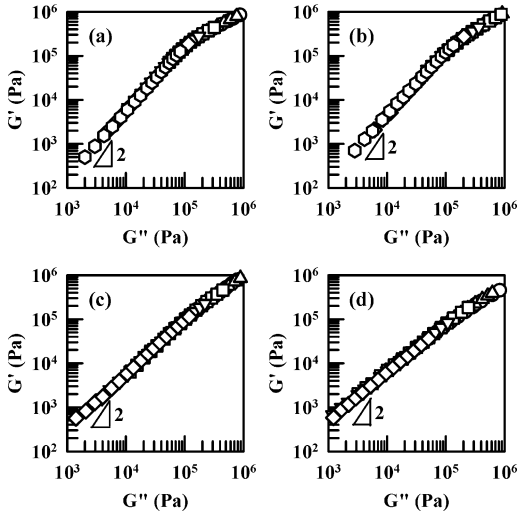

Figure 11. Log G' vs log G'' plots for: (a) 20/80 PVPh/PVAc blend at different temperatures (°C): (○) 74, (△) 84, (□) 94, (▽) 104, (◇) 114 and, (⬠) 124; (b) 40/60 blend at different temperatures (°C): (○) 100, (△) 110, (□) 120, (▽) 130, (◇) 140, and (⬠) 150; (c) 60/40 blend at different temperatures (°C): (○) 131, (△) 141, (□) 151, (▽) 161, and (◇) 171; (d) 80/20 blend at different temperatures (°C): (○) 162, (△) 172, (□) 182, (▽) 192, and (◇) 202.

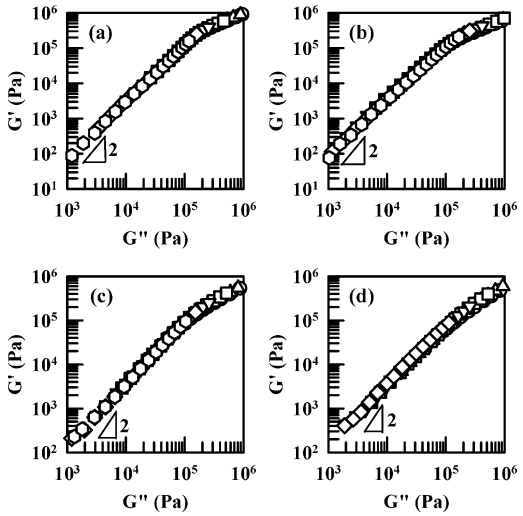

Figure 12. Log G' vs log G'' plots for: (a) 20/80 PVPh/PVME blend at different temperatures (°C): (○) 29, (△) 39, (□) 49, (▽) 59, (◇) 69, and (⬠) 79; (b) 40/60 PVPh/PVME blend at different temperatures (°C): (○) 54, (△) 64, (□) 74, (▽) 84, (◇) 94, and (⬠) 104; (c) 60/40 PVPh/PVME blend at different temperatures (°C): (○) 102, (△) 112, (□) 122, (▽) 132, (◇) 142, and (⬠) 152; (d) 80/20 PVPh/PVME blend at different temperatures (°C): (○) 136, (△) 146, (□) 156, (▽) 166, and (◇) 176.

(b) Log G' vs log G'' Plots, Composition Fluctuations, and Time−Temperature Superposition. Log G' vs log G'' plots at various temperatures are given in Figure 11 for PVPh/PVAc blends, in Figure 12 for PVPh/PVME blends, in Figure 13 for PVPh/P2VP blends, and in Figure 14 for PVPh/P4VP blends. In Figures 11−14 there are three common features in all four PVPh-based miscible polymer blend systems: (1) log G' vs log G'' plots are independent of temperature over the entire range of temperatures investigated, (2) the curvature of log G' vs log G'' plots in the terminal region becomes progressively pronounced as the amount of PVPh in each blend is increased from 20 to 80 wt %, and (3) the temperature independence of log G' vs log G'' plots is very similar to the corresponding log G' vs log $a_T\omega$ plots, especially in the terminal region.

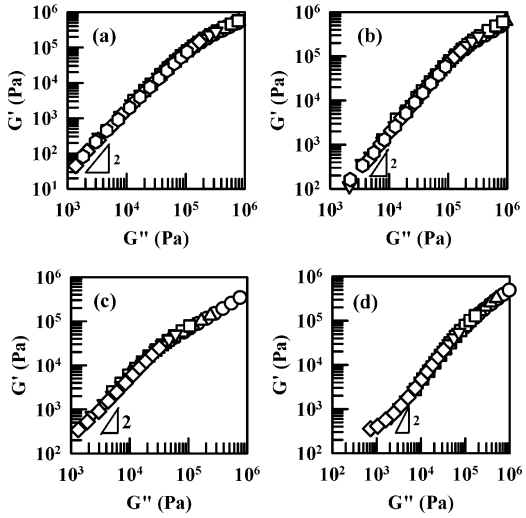

Figure 13. Plots of log G' vs log G'' for: (a) 20/80 PVPh/P2VP blend at different temperatures (°C): (○) 151, (△) 161, (□) 171, (▽) 181, (◇) 191, and (⬡) 201; (b) 40/60 PVPh/P2VP blend at different temperatures (°C): (○) 176, (△) 186, (□) 196, (▽) 206, (◇) 216, and (⬡) 226; (c) 60/40 blend at different temperatures (°C): (○) 191, (△) 201, (□) 211, (▽) 221, and (◇) 231; (d) 80/20 blend at different temperatures (°C): (○) 201, (△) 211, (□) 221, (▽) 231, and (◇) 241.

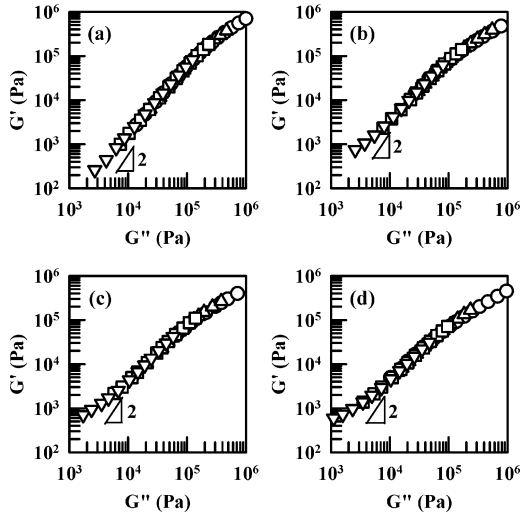

Figure 14. Plots of log G' vs log G'' for PVPh/P4VP blends annealed at 200 °C for 3 h: (a) 20/80 PVPh/P4VP blend at different temperatures (°C): (○) 209, (△) 219 (□) 229, ad (▽) 239; (b) 40/60 PVPh/P4VP blend at different temperatures (°C): (○) 216, (△) 226, (□) 236, and (▽) 246; (c) 60/40 PVPh/P4VP blend at different temperatures (°C): (○) 222, (△) 232, (□) 242, and (▽) 252; (d) 80/20 PVPh/P4VP blend at different temperatures (°C): (○) 216, (△) 226, (□) 236, and (▽) 246.

Let us consider the origin of curvature in the terminal region of log G' vs log G'' plots given in Figures 11−14. The factors that could have caused curvature in the terminal region of log G' vs log G'' plots are (1) cross-linking, (2) dynamic heterogeneity, and (3) intermolecular attractive interaction (hydrogen bonding). If there had any cross-linking in any of the four PVPh-based miscible blends, temperature-independent log G' vs log G'' pots could not have obtained and thus TTS should have failed. However, from Figures 11−14 we can conclude that TTS works for all four PVPh-based blend systems. Therefore, cross-linking of PVPh cannot be a reason for the curvature in the terminal region of log G' vs log G'' plots. It was reported that the PVPh/P4VP blends, for instance, were miscible even on the scale of 2−3 nm,[71] suggesting that dynamic heterogeneity may not be a source that gives rise to the curvature observed in the terminal region of log G' vs log G'' plots. Then, the curvature in the terminal region of log G' vs log G'' plots is attributable to the presence of intermolecular attractive interactions (hydrogen bonding) in the PVPh-based miscible blend systems investigated in this study.

Recall that referring to Figure 4 for neat PVPh, we attributed the curvature in the terminal region of log G' vs log G'' plots to the self-association of phenolic −OH groups in PVPh (see Figure 1 for FTIR spectrum of PVPh). According to Han and co-workers,[78,79] the temperature independence of log G' vs log G'' plots signifies little or no morphological change occurring in a polymer (or polymer blend) over the range of temperatures investigated, while log G' vs log G'' plots are expected not only to be independent of temperature but also to have a slope of 2 in the terminal region for all homogeneous polymeric liquids including the block copolymers in the disordered state and the liquid-crystalline polymers in the isotropic state. Previously, Ajii et al.[16,17] reported that log G' vs log G'' plots in the terminal region of PS/PVME blends, which exhibit lower critical separation temperature (LCST) behavior, had little or no temperature dependence at temperatures below LCST (i.e., in the homogeneous state) but had a strong temperature dependence at temperatures above LCST (i.e., in the immiscible state). Nonetheless, the log G' vs log G'' plots in the terminal region for the homogeneous state of PS/PVME blends had a slope much less than 2, which was attributed to significant concentration fluctuations and dynamic heterogeneity. However, the presence of curvature in the terminal region of log G' vs log G'' plots for the four PVPh-based miscible blends investigated in this study must have a different origin because TTS works for those blends, and thus significant concentration fluctuations and dynamic heterogeneity might have not occurred in those blends. In other words, the origin of curvature in the terminal region of log G' vs log G'' plots for the four PVPh-based miscible blends is attributable to the presence of strong intermolecular attractive interactions (hydrogen bonding).

It is appropriate to discuss at this juncture the previous rheological studies on PVPh-based miscible polymer blends. Akiba and Akiyama[75] reported on the linear dynamic viscoelasticity of PVPh/PVME and PS/PVME blend systems. They observed that log a_T vs $T - T_r$ plots were virtually identical, and the slope of log G' vs log $a_T\omega$ plots in the terminal region was 2 for both PVPh/PVME and PS/PVME blend systems, in spite of the fact that PVPh/PVME blends are expected to form hydrogen bonds (see, for instance, Figure 5a in this paper). However, Akiba and Akiyama did not present FTIR spectra of the PVPh/PVME blends employed. That is, the study of Akiba and Akiyama did not reveal any difference in linear dynamic viscoelasticity between PS/PVME blends without specific interaction and PVPh/PVME blends with specific interactions.

In this study, we compared the linear dynamic viscoelasticity between PVPh/PVME blends and PS/PVME blends. Figure 15 gives (a) log G' vs log $a_T\omega$ plots and (b) log G' vs log G'' plots for 60/40 PVPh/PVME blend at various temperatures ranging from 102 to 162 °C (the open symbols) and for 60/40 PS/PVME blend at various temperatures ranging from 58 to 98 °C (the filled symbols). It should be mentioned that the binodal curve for the PS/PVME blends, which exhibit lower critical temperature (LCST), lies far above 98 °C. It is clearly seen in Figure 15 that the linear dynamic viscoelasticity between the two blends are quite different while both blends show temperature independence. First, both log G' vs log $a_T\omega$ and log G' vs log G'' plots of 60/40 PVPh/PVME blend do not overlap those of 60/40 PS/PVME blend, clearly at odds with the results reported

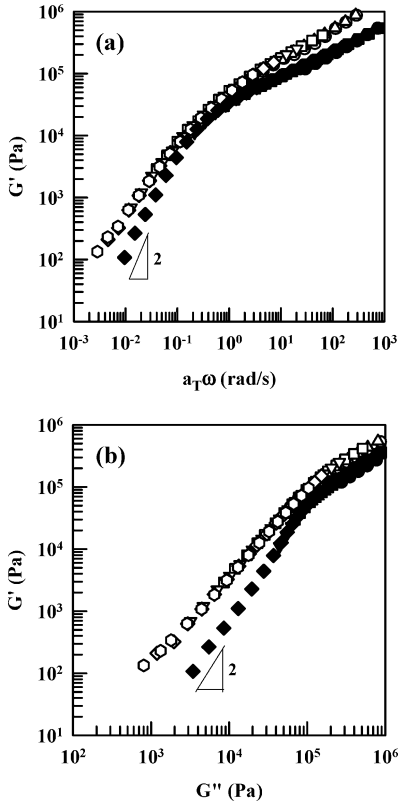

Figure 15. (a) Log G' vs log $a_T\omega$ plots with $T_r = T_{gm} + 50$ °C as the reference temperature for 60/40 PVPh/PVME blend at various temperatures (°C): (○) 102, (△) 122, (□) 132, (▽) 142, (◇) 152, and (⬠) 162, and for 60/40 PS/PVME blend at various temperatures (°C): (●) 58, (▲) 68, (■) 78, (▼) 88, and (◆) 98. (b) Log G' vs log G'' plots for 60/40 PVPh/PVME blend at various temperatures (°C): (○) 102, (△) 122, (□) 132, (▽) 142, (◇) 152, and (⬠) 162, and for 60/40 PS/PVME blend at various temperatures (°C): (●) 58, (▲) 68, (■) 78, (▼) 88, and (◆) 98.

by Akiba and Akiyama.[75] Next, in the terminal region of both log G' vs log $a_T\omega$ and log G' vs log G'' plots the 60/40 PS/PVME blend has a slope very close to 2 (the filled symbols), whereas the 60/40 PVPh/PVME blend shows curvature (the open symbols). The obvious differences between the present study and the previous study of Akiba and Akiyama[75] are the molecular weights of the polymers employed; namely in the study of Akiba and Akiyama[75] $M_w = 5.0 \times 10^3$ for PVPh, $M_w = 7.42 \times 10^4$ for PVME, and $M_w = 5.0 \times 10^3$ for PS, while in the present study $M_w = 2.16 \times 10^4$ for PVPh, $M_w = 1.64 \times 10^5$ for PVME, and $M_w = 1.32 \times 10^5$ for PS. Nonetheless, we cannot reconcile the differences observed in both log G' vs log $a_T\omega$ and log G' vs log G'' plots between the two studies. It should be pointed out that log G' vs log G'' plots are expected to be independent not only of temperature but also independent of molecular weight for entangled homopolymers.[100] In the present study we have presented, via FTIR spectra (see Figure 5a), clear evidence of the formation of hydrogen bonds between the constituent components in the PVPh/PVME blends employed. Note that no specific interaction is expected between PS and PVME in PS/PVME blend.

Cai et al.[76] reported the linear dynamic viscoelasticity of PVPh/PEO blends. Note that PVPh and PEO are known to be miscible for PEO content less than about 60 wt % and form hydrogen bonds.[68,101] Cai et al. observed that plots of log G' vs log $a_T\omega$ and log G'' vs log $a_T\omega$ with $T_r = T_{gm} + 15$ °C was independent of temperature and the slope of log G' vs log $a_T\omega$ plots in the terminal region was much smaller than 2. Such experimental results are very similar to those (see Figure 10)

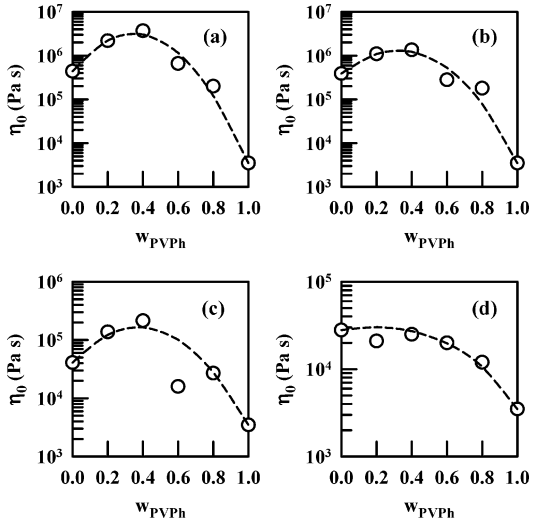

Figure 16. Plots of log η_0 vs weight fraction of PVPh (w_{PVPh}) at $T = T_{gm} + 50$ °C for (a) PVPh/PVAc blend system, (b) PVPh/PVME blend system, (c) PVPh/P2VP blend system, and (d) VPh/P4VP blend system.

obtained for the four PVPh-based miscible polymer blend systems investigated in the present study. However, Cai et al. reported that plots of zero-shear viscosity ($\eta_{0,b}$) vs blend composition prepared at $T_r = T_g + 15$ °C went through a maximum at a weight fraction of PEO (w_{PEO}) of about 0.2 and then a minimum at $w_{PEO} \approx 0.25$.

Figure 16 gives plots of log $\eta_{0,b}$ vs weight fraction of PVPh (w_{PVPh}) prepared at $T_r = T_g + 50$ °C for all four PVPh-based miscible blends investigated in the present study. In Figure 16 we do not observe any abnormality in the composition dependence of $\eta_{0,b}$ for the PVPh-based miscible blends, in contrast to the results reported by Cai et al.[76] We are of the opinion that the seemingly anomalous composition dependence of $\eta_{0,b}$ of the PVPh/PEO blends observed by Cai et al. might be attributable to the choice of T_r very close to the T_g of the blends, i.e., $T_r = T_g + 15$ °C.

4. Concluding Remarks

In this paper we have presented experimental results for the linear dynamic viscoelasticity of four PVPh-based miscible polymer blend systems with hydrogen bonding. We have confirmed that each of the blend systems investigated formed hydrogen bonding between the constituent components as determined by FTIR spectroscopy. We have found that the self-association of the phenolic −OH groups in PVPh and the interassociation (intermolecular attractive interactions) between the constituent components have a profound influence on the linear dynamic viscoelasticity of the respective blend systems.

We have found that log G' vs log $a_T\omega$ and log G'' vs log $a_T\omega$ plots and also log G' vs log G'' plots for all four PVPh-based blend systems show temperature independence. Further, we have found that plots of log $a_T\omega$ vs $T - T_r$ with T_r being a reference temperature show composition independence in all four PVPh-based blend system investigated, in spite of very large differences in the component glass transition temperatures of the constituent components (ΔT_g), including the PVPh/PVME blend system having the value of ΔT_g as large as 199 °C. Therefore, we conclude that an application of TTS is warranted for the four PVPh-based miscible blend systems with hydrogen bonding. If we apply the same empirical criterion, which has been applied to miscible polymer blends without specific interaction (see the Introduction), to the four PVPh-based miscible polymer blends investigated in this study, we can

conclude that the effects of concentration fluctuations and dynamic heterogeneity on the rheological behavior of the miscible polymer blends might be very small, if not negligible. This conclusion is a distinguishing rheological characteristic between the miscible polymer blends with specific interaction (hydrogen bonding in the present study) and the miscible polymer blends without specific interaction. The apparent absence or negligibly small concentration fluctuations and dynamic heterogeneity in the four PVPh-based miscible polymer blend systems with hydrogen bonding can be attributed to the presence of self-association (intramolecular interactions) and/or interassociation (intermolecular attractive interactions) between the constituent components. It seems very reasonable to speculate that strong intermolecular attractive interactions would suppress concentration fluctuations in miscible polymer blends forming hydrogen bonds.

However, we have observed curvature in the terminal region of log G' vs log G'' plots for all four PVPh-based blend systems investigated, and the severity of curvature becomes more pronounced as the concentration of PVPh in the respective blend systems is increased. Specifically, for blends with low concentrations of PVPh (e.g., 20 wt %), since PVPh is surrounded by large amounts of non-self-associating component, the fraction of self-association of phenolic −OH groups would be very small, and thus most of the phenolic −OH groups form the intermolecular hydrogen bonds and the blends are miscible. However, because of the low concentration of PVPh, the number of hydrogen bonds in such blends may not be sufficiently large. We have shown (see Table 5) that the fraction of hydrogen-bonded phenolic groups (−OH) is small (about 20%). As a result, the effect of specific interactions on the linear dynamic viscoelasticity would be small, and consequently the curvature in the terminal region of log G' vs log G'' plots is not discernible. However, as the concentration of PVPh is increased, there are not only intermolecular hydrogen bonding but also self-association of phenolic −OH groups. Hydrogen-bonding enhances the friction between different segments. Thus, very strong intermolecular interactions between the constituent components in such miscible polymer blends may suppress concentration fluctuations and dynamic heterogeneity. It can then be concluded that the curvature in the terminal region of log G' vs log G'' plots is attributable to both self-association and interassociation in PVPh-based miscible polymer blends when concentration of PVPh exceeds a certain critical value.

It is worth mentioning that the balance between self-association and interassociation in miscible polymer blends with hydrogen-bonding would vary depending on their relative strength of hydrogen bonding. Let us consider, for illustration, the 60/40 PVPh/PVME blend. From the calculation of the fraction of hydrogen bonds in this blend, we find that about 46% of the ether groups in PVME are associated with the phenolic −OH group in PVPh (see Table 5). In addition, the fraction of self-associated phenolic −OH groups is about 59%, which is much larger than the fraction (about 38%) of interassociated phenolic −OH groups. (These values are calculated from Table 5 under the assumption that the mole fraction of functional groups is equal to the weight fraction of the constituent components.) It can then be concluded that the predominant hydrogen bonding in this blend arises from self-association. As a result, the curvature in the terminal region of log G' vs log G'' plots for the 60/40 PVPh/PVME blend is attributable primarily to the self-association of PVPh rather than interassociation in the blend.

On the other hand, we know from the FTIR spectra (see Figure 5) and the composition dependence of T_g (see Figure 7) that P4VP forms stronger intermolecular hydrogen bonds with PVPh, for example, in 60/40 PVPh/P4VP blend than with PVME in 60/40 PVPh/PVME blends. From the calculation of the fraction of hydrogen bonds formed in the 60/40 PVPh/P4VP blend, we find that about 80% (see Table 5) of the pyridine groups in P4VP are associated with the phenolic −OH groups in PVPh. Further, the fraction of self-associated phenolic −OH groups in 60/40 PVPh/P4VP blend is only about 38%, and about 53% of phenolic −OH groups in PVPh is hydrogen-bonded with the pyridine groups in P4VP. As a result, the curvature in the terminal region of log G' vs log G'' plots of 60/40 PVPh/P4VP blend is attributable primarily to the interassociation (intermolecular hydrogen bonding) between the phenolic −OH groups in PVPh and the pyridine groups in P4VP, although some self-association is also involved. Similar arguments can be made to PVPh/PVAc and PVPh/P2VP blend systems investigated in this study.

In summary, for the first time, we have presented experimental results, demonstrating clearly a distinction in linear dynamic viscoelasticity between the miscible polymer blends with specific interaction (hydrogen bonding in the present study) and the miscible polymer blends without specific interaction.

Supporting Information Available: Summary of the Coleman−Graf−Painter association model for the analysis of hydrogen bonding in miscible polymer blends with specific interactions; summary of the thermodynamic theory of Painter and co-workers for predicting the composition dependence of glass transition temperature of miscible polymer blends with specific interactions; enlarged plots of log G' vs log $a_T\omega$ and log G'' vs log $a_T\omega$ plots for 60/40 PVPh/PVME and 60/40 PVPh/P2VP blends at various temperatures; plots of loss angle vs reduced angular frequency (i.e., log tan δ vs log $a_T\omega$ plots), together with log G' vs log $a_T\omega$ and log G'' vs log $a_T\omega$ plots, for the four PVPh-based miscible polymer blend systems investigated in this study. The material is available free of charge via the Internet at http://pubs.acs.org.

References and Notes

(1) Israelachvili, J. N. *Intermolecular and Surface Forces*, 2nd ed.; Academic Press: New York, 1991.
(2) Huyskens, P. L., Luck, W. A. P., Zeegers-Huyskens, T., Eds.; *Intermolecular Forces*; Springer-Verlag: New York, 1991.
(3) Prest, W. M.; Porter, R. S. *J. Polym. Sci., Part A2* **1972**, *10*, 1639.
(4) Stadler, R.; de Araujo, M. A. *Makromol. Chem., Macromol. Symp.* **1990**, *38*, 243.
(5) Kim, J. K.; Han, C. D.; Lee, Y. J. *Polym. J.* **1992**, *24*, 205.
(6) Colby, R. H. *Polymer* **1989**, *30*, 1275.
(7) Lyngaae-Jorgensen, J.; Sondergaard, K. *Polym. Eng. Sci.* **1987**, *27*, 351.
(8) Wu, S. *Polymer* **1987**, *28*, 1144.
(9) Han, C. D.; Kim, J. K. *Macromolecules* **1989**, *22*, 1914.
(10) Han, C. D.; Kim, J. K. *Macromolecules* **1989**, *22*, 4292.
(11) Yang, H. H.; Han, C. D.; Kim, J. K. *Polymer* **1994**, *35*, 1503.
(12) Kim, E.; Kramer, E. J.; Wu, W. C.; Garrett, P. D. *Polymer* **1994**, *35*, 5706.
(13) Pathak, J. A.; Colby, R. H.; Klamath, S. Y.; Kumar, S.; Staler, R. *Macromolecules* **1998**, *31*, 8988.
(14) Aoki, Y.; Tanaka, T. *Macromolecules* **1999**, *32*, 8560.
(15) Wu, S. *J. Polym. Sci., Polym. Phys. Ed.* **1987**, *25*, 557.
(16) Ajji, A.; Choplin, L.; Prud'homme, R. E. *J. Polym. Sci., Polym. Phys. Ed.* **1988**, *26*, 2279.
(17) Ajji, A.; Choplin, L.; Prud'Homme, R. E. *J. Polym. Sci., Polym. Phys. Ed.* **1991**, *29*, 1573.
(18) Schneider, H. A.; Wirbser, J. *New Polym. Mater.* **1990**, *2*, 149.
(19) Green, P. F.; Adolf, D. B.; Gilliom, L. R. *Macromolecules* **1991**, *24*, 3377.
(20) Roland, C. M.; Ngai, K. L. *Macromolecules* **1992**, *25*, 363.
(21) Kapnistos, M.; Hinrichs, A.; Vlassopoulos, D.; Anastasiadis, S. H.; Stammer, A.; Wolf, B. A. *Macromolecules* **1996**, *29*, 7155.
(22) Kim, J. K.; Lee, H. H.; Son, H. W.; Han, C. D. *Macromolecules* **1998**, *31*, 8566.

(23) Pathak, J. A.; Colby, R. H.; Floudas, G.; Jerome, R. *Macromolecules* **1999**, *32*, 2553.
(24) Stadler, R.; de Lucca, Freitas, L.; Krieger, V.; Klotz, S. *Polymer* **1988**, *29*, 1643.
(25) Ajji, A.; Choplin, L. *Macromolecules* **1991**, *24*, 5221.
(26) Cavaille, J. Y.; Perez, J.; Jourdan, C.; Johari, G. P. *J. Polym. Sci., Polym. Phys. Ed.* **1987**, *25*, 1847.
(27) Takahashi, Y.; Suzuki, H.; Nakagawa, Y.; Noda, I. *Macromolecules* **1994**, *27*, 6476.
(28) Kitade, S.; Takahashi, Y.; Noda, I. *Macromolecules* **1994**, *27*, 7397.
(29) Roland, C. M.; Ngai, K. L. *Macromolecules* **1991**, *24*, 2261.
(30) Chung, G. C.; Kornfield, J. A.; Smith, S. D. *Macromolecules* **1994**, *27*, 5729.
(31) Arendt, B. H.; Krishnamoorti, R.; Kornfield, J. A.; Smith, S. D. *Macromolecules* **1997**, *30*, 1127.
(32) Trask, C. A.; Roland, C. M. *Macromolecules* **1989**, *22*, 256.
(33) Roovers, J.; Toporowski, P. M. *Macromolecules* **1992**, *25*, 3454.
(34) Zawada, J. A.; Fuller, G. G.; Colby, R. H.; Fetters, L. J.; Roovers, J. *Macromolecules* **1994**, *27*, 6861.
(35) Ngai, K. L.; Plazek, D. J. *Macromolecules* **1990**, *23*, 4282.
(36) Alegria, A.; Elizetxea, C.; Cendoya, I.; Colmenero, J. *Macromolecules* **1995**, *28*, 8819.
(37) Friedrich, C.; Schwarzwaelder, C.; Riemann, R. E. *Polymer* **1996**, *37*, 2499.
(38) Wendorff, J. H. *J. Polym. Sci., Polym. Lett. Ed.* **1980**, *18*, 439.
(39) Miller, J. B.; McGrath, K. J.; Roland, C. M.; Trask, C. A.; Garroway, A. N. *Macromolecules* **1990**, *23*, 4543.
(40) Roovers, J.; Toporowski, P. M. *Macromolecules* **1992**, *25*, 1096.
(41) Chung, G. C.; Kornfield, J. A.; Smith, S. D. *Macromolecules* **1994**, *27*, 964.
(42) Muller, G.; Stadler, R.; Schlick, S. *Macromolecules* **1994**, *27*, 1555.
(43) Katana, G.; Fischer, E. W.; Hack, T.; Abetz, V.; Kremer, F. *Macromolecules* **1995**, *28*, 2714.
(44) Zetsche, A.; Fischer, E. W. *Acta Polym.* **1994**, *45*, 168.
(45) Kumar, S. K.; Colby, R. H.; Anastasiadis, S. H.; Fytas, G. *J. Chem. Phys.* **1996**, *105*, 3777.
(46) Muller, G.; Stadler, R.; Schlick, S. *Makromol. Chem., Rapid Commun.* **1992**, *13*, 117.
(47) Cendoya, I.; Alegria, A.; Alberdi, J. M.; Colmenero, J.; Grimm, H.; Richter, D.; Frick, B. *Macromolecules* **1999**, *32*, 4065.
(48) Schmidt-Rohr, K.; Clauss, J.; Spiess, H. W. *Macromolecules* **1992**, *25*, 3273.
(49) Le, Menestrel, C.; Kenwright, A. M.; Sergot, P.; Laupretre, F.; Monnerie, L. *Macromolecules* **1992**, *25*, 3020.
(50) Wagler, T.; Rinaldi, P. L.; Han, C. D.; Chun, H. *Macromolecules* **2000**, *33*, 1778.
(51) Shimizu, H.; Horiuchi, S.; Kitano, T. *Macromolecules* **1999**, *32*, 537.
(52) Coleman, M. M.; Graf, J. F.; Painter, P. C. *Specific Interactions and the Miscibility of Polymer Blends*; Technomic Publishing: Lancaster, PA, 1991.
(53) Zhang, S. H.; Jin, X.; Painter, P. C.; Runt, J. *Polymer* **2004**, *45*, 3933.
(54) Pedrosa, P.; Pomposo, J. A.; Calahorra, E.; Cortazar, M. *Macromolecules* **1994**, *27*, 102.
(55) Lezcano, E. G.; De Arellano, D. R.; Prolongo, M. G.; Coll, C. S. *Polymer* **1998**, *39*, 1583.
(56) Zhang, S.; Jin, X.; Painter, P. C.; Runt, J. *Macromolecules* **2002**, *35*, 3636.
(57) Serman, C. J.; Painter, P. C.; Coleman, M. M. *Polymer* **1991**, *32*, 1049.
(58) Meaurio, E.; Zuza, E.; Sarasua, J.-R. *Macromolecules* **2005**, *38*, 1207.
(59) Moskala, E. J.; Howe, S. E.; Painter, P. C.; Coleman, M. M. *Macromolecules* **1984**, *17*, 1671.
(60) Coleman, M. M.; Lichkus, A. M.; Painter, P. C. *Macromolecules* **1989**, *22*, 586.
(61) Serman, C. J.; Xu, Y.; Painter, P. C.; Coleman, M. M. *Polymer* **1991**, *32*, 516.
(62) Zhang, S.; Painter, P. C.; Runt, J. *Macromolecules* **2002**, *35*, 8478.
(63) Zhang, S. H.; Jin, X.; Painter, P. C.; Runt, J. *Macromolecules* **2002**, *35*, 9403.
(64) Iriondo, P.; Iruin, J. J.; Fernandez-Berridi, M. J. *Macromolecules* **1996**, *29*, 5605.
(65) Hill, D. J. T.; Whittaker, A. K.; Wong, K. W. *Macromolecules* **1999**, *32*, 5285.
(66) Chen, H. L.; Liu, H. H.; Lin, J. S. *Macromolecules* **2000**, *33*, 4856.
(67) Goh, S. H.; Lee, S. Y.; Luo, X.; Wong, M. W.; Tan, K. L. *Macromol. Chem. Phys.* **2001**, *202*, 31.
(68) Sotele, J. J.; Soldi, V.; Pires, A. T. N. *Polymer* **1997**, *38*, 1179.
(69) Zhang, S.; Painter, P. C.; Runt, J. *Macromolecules* **2004**, *37*, 2636.
(70) Vivas, de Meftahia, M.; Frechet, J. M. J. *Polymer* **1988**, *29*, 477.
(71) Wang, J.; Cheung, M. K.; Mi, Y. *Polymer* **2001**, *42*, 3087.
(72) Cesteros, L. C.; Isasi, J. R.; Katime, I. *Macromolecules* **1993**, *26*, 7256.
(73) Cesteros, L. C.; Meaurio, E.; Katime, I. *Macromolecules* **1993**, *26*, 2323.
(74) Kuo, S. W.; Chang, F. C. *Macromolecules* **2001**, *34*, 5224.
(75) Akiba, I.; Akiyama, S. *Polym. Networks Blends* **1997**, *7*, 147.
(76) Cai, H.; Ait-Kadi, A.; Brisson, J. *Polymer* **2003**, *44*, 1481.
(77) Still, R. H.; Whitehead, A. *J. Appl. Polym. Sci.* **1977**, *21*, 1199.
(78) (a) Han, C. D.; Kim, J. *J. Polym. Sci., Polym. Phys. Ed.* **1987**, *25*, 1741. (b) Han, C. D.; Kim, J.; Kim, J. K. *Macromolecules* **1989**, *22*, 383. (c) Han, C. D.; Baek, D. M.; Kim, J. K. *Macromolecules* **1990**, *23*, 561. (d) Yoon, P. V.; Han, C. D. *Macromolecules* **2000**, *33*, 2171.
(79) (a) Kim, S. S.; Han, C. D. *Macromolecules* **1993**, *26*, 6633. (b) Kim, S. S.; Han, C. D. *Polymer* **1994**, *35*, 93. (c) Han, C. D.; Kim, S. S. *Macromolecules* **1995**, *28*, 2089.
(80) Dai, J.; Goh, S. H.; Lee, S. Y.; Siow, K. S. *Polym. J.* **1994**, *26*, 905.
(81) Whetsel, K. B.; Lady, J. H. In *Spectrometry of Fuels*, Friedel, H., Ed.; Plenum Press: New York, 1970; p 273.
(82) Zhang, H. X.; Bhagwagar, D. E.; Graf, J. F.; Painter, P. C.; Coleman, M. M. *Polymer* **1994**, *35*, 5379.
(83) Painter, P. C.; Graf, J. F.; Coleman, M. M. *Macromolecules* **1991**, *24*, 5630.
(84) Gramstad, T. *Acta Chem. Scand.* **1962**, *16*, 807.
(85) Chandra, A. K.; Banerjee, S. *J. Phys. Chem.* **1962**, *66*, 952.
(86) Rubin, J.; Senkowski, B. Z.; Panson, G. S. *J. Phys. Chem.* **1964**, *68*, 1601.
(87) Rubin, J.; Panson, G. S. *J. Phys. Chem.* **1965**, *69*, 3089.
(88) Hopkins, H. P.; Alexander, C. J.; All, S. Z. *J. Phys. Chem.* **1978**, *82*, 1268.
(89) Gordon, M.; Taylor, J. S. *J. Appl. Chem* **1952**, *2*, 493.
(90) Fox, T. G. *Bull. Am. Phys. Soc.* **1956**, *1*, 123.
(91) Couchman, P. R. *Macromolecules* **1978**, *11*, 1156.
(92) Couchman, P. R.; Karasz, F. E. *Macromolecules* **1978**, *11*, 117.
(93) Couchman, P. R. *Polym. Eng. Sci.* **1984**, *24*, 135.
(94) Kwei, T. K. *J. Polym. Sci., Polym. Lett. Ed.* **1984**, *22*, 307.
(95) Kwei, T. K.; Pearce, E. M.; Pennacchia, J. R.; Charton, M. *Macromolecules* **1987**, *20*, 1174.
(96) Kim, J. H.; Min, B. R.; Kang, Y. S. *Macromolecules* **2006**, *39*, 1297.
(97) Lu, X.; Weiss, R. A. *Macromolecules* **1992**, *25*, 3242.
(98) van Krevelen, D. W. *Properties of Polymers*, 3rd ed.; Elsevier: Amsterdam, 1990; p 109.
(99) Ferry, J. D. *Viscoelastic Properties of Polymers*, 3rd ed.; Wiley: New York, 1980.
(100) (a) Han, C. D.; Jhon, M. S. *J. Appl. Polym. Sci.* **1986**, *32*, 3809. (b) Han, C. D. *J. Appl. Polym. Sci.* **1988**, *35*, 167. (c) Han, C. D.; Kim, J. K. *Polymer* **1993**, *34*, 2533.
(101) Zhang, X.; Takegoshi, K.; Hikichi, K. *Macromolecules* **1992**, *25*, 2336.

MA7025385